RUMPH, CANDIE, M.S. Aberrant DNA Methylation and Patterns of Histone Modifications at the WNT5A Promoter B in Osteosarcoma Cells. (2014) Directed by Dr. Karen Katula. 60 pp.

WNT5A is a secreted ligand involved in differentiation, proliferation, cell movement and apoptosis. WNT5A is often misregulated in cancer and is known to be involved in cancer metastasis. The focus of this study was the possible epigenetic regulation of *WNT5A* expression in osteosarcoma cells. I analyzed *WNT5A* regulation from its two major transcription start sites, termed Promoter A and Promoter B. The levels of promoter B transcripts were reduced in the osteosarcoma cell line, U20S, and in primary osteosarcoma tissue of three individuals, compared to normal osteoblasts. To determine if this decrease in Promoter B activity in U20S is due to DNA methylation, I analyzed six CpG islands associated with Promoter B by bisulfite sequencing. Results show that Regions 1 and 2 are unmethylated, Regions 3, 4, 5 are methylated and Region 6, which includes the Promoter B start of transcription, is partially methylated. The DNA methylation pattern is similar to the pattern determined in another osteosarcoma cell line, SaOS-2. Region 6, however, is only 25% methylated in U20S, whereas 62% methylated in SaOS-2. The level of methylation is negatively correlated with Promoter B transcript levels, indicating that Region 6 methylation decreases transcription. Histone modifications were examined for their involvement in Promoter A and Promoter B activity by chromatin immunoprecipitation (ChIP) assays. H3K4me3, an activating histone mark, was highly enriched in Promoter A and reduced in Promoter B Region 6 of U20S cells, indicating that H3K4me3 has a role in the reduction of Promoter B activity. H3K27me3 and H3K9me3, repressive histone marks, were not differentially altered on

Promoters A and B. H3K27me3 was enriched on Regions 3 and 4 located upstream of the Promoter B start of transcription. Overall, these results suggest that *WNT5A* Promoter B activity is reduced in osteosarcoma as a result of both histone modification and DNA methylation.

ABERRANT DNA METHYLATION AND PATTERNS OF HISTONE MODIFICATIONS AT THE WNT5A PROMOTER B IN OSTEOSARCOMA CELLS

by

Candie Rumph

A Thesis Submitted to
the Faculty of The Graduate School at
The University of North Carolina at Greensboro
in Partial Fulfillment
of the Requirements for the Degree
Master of Science

Greensboro
2014

Approved by

_____
Committee Chair

To my family and friends, for their love, support and encouragement through this journey.

APPROVAL PAGE

This thesis written by Candie Rumph has been approved by the following committee of the Faculty of The Graduate School at The University of North Carolina at Greensboro.

Committee Chair _____

Committee Members _____

_____

_____
Date of Acceptance by Committee

_____
Date of Final Oral Examination

ACKNOWLEDGEMENTS

First, I would like to thank Dr. Karen Katula, for her patience, direction and guidance for my graduate research project. I would like to show my appreciation to my committee members, Dr. Amy Adamson and Dr. John Tomkiel for their time and serving on my committee. I would also like to thank former members of the lab, Nicole Joyner-Powell, Judy Hsu, and Himani Vaidya for their previous contributions to make my research possible.

Lastly, I would like to thank my family for their support and encouragement in my present and future endeavors.

TABLE OF CONTENTS

Page

LIST OF TABLES

Page

LIST OF FIGURES

Page

CHAPTER I

INTRODUCTION

The American Cancer Society (2012) estimates that one half of men and one third of women in the United States will get cancer. The general feature of many cancers is that cells grow uncontrollably and may eventually metastasize. These cellular characteristics are caused by genetic and non genetic changes. *WNT5A* is a gene that is often misregulated in cancer by non genetic or epigenetic changes. Significantly, WNT5A has been shown to be involved in cancer cell metastasis. The human *WNT5A* gene gives rise to two different protein isoforms due to distinct transcriptional start sites (we termed Promoter A and Promoter B). Studies of *WNT5A* gene methylation mostly have focused on the Promoter A region but sequence analysis shows that Promoter B also contains CpG islands. The goals of this project were to determine the Promoter A and Promoter B transcript levels and to analyze methylation status of the Promoter B associated CpG islands in osteosarcoma cells. In addition, specific histone modifications associated with *WNT5A* Promoter A and Promoter B were analyzed. These data suggest a mechanism for the alteration of WNT5A expression during cancer progression.

WNT5A Signaling

The Wnts are a family of secreted glycoproteins responsible for regulation of cell proliferation, differentiation, cell movement, and apoptosis. Wnt glycoproteins perform these functions by interacting with the Frizzled cell surface receptors (Fz) (Clevers, 2006). Wnt signaling operates through two different pathways, the canonical and non canonical. The canonical pathway is a beta-catenin-dependent path that involves Wnt protein binding to lipoprotein receptor (Lpr) and the Fz receptor (MacDonald et al., 2009). This leads to the recruitment of the "Axin complex" that normally targets beta-catenin for proteasome degradation (Clevers, 2006). The axin complex includes the following proteins: glycogen synthase kinase 3(GSK3), adenomatous polyposis (APC), casein kinase 1 (CK1) and axin (MacDonald et al., 2009). Active beta-catenin moves to the nucleus and binds to T-Cell factor/lymphoid enhancer factor (Tcf/Lef). This beta-catenin-Tcf/lef complex acts as a transcription factor activating transcription of target genes such as *myc* (ten Berge et al., 2008) and *cyclin D* (Sansom et al., 2005). WNT5A does not directly signal through the canonical pathway but can negatively affect the cannonical beta-catenin pathway (Figure 1).

WNT5A signals through the non-canonical pathway. The non-canonical pathway involves signaling through the Fz and Ror1/2 receptors and does not lead to beta-catenin activation but rather initiates either the RhoA/Rac or calcium (Ca^{2+}) pathways. WNT5A forms a tertiary complex with the Fz and Ror1/2 receptors. The activated Fz receptor leads to phosphorylation of Dishevelled (Dvl). Dvl signals guanosine nucleotide-binding

proteins (G proteins), RhoA and Rac. RhoA leads to activation of Rho-kinase and Rac leads to activation of JNK (c-Jun N-terminal kinase). Rho kinase and JNK both lead to cytoskeletal changes, affecting cell polarity and migration. The other non-canonical pathway that WNT5A regulates is the Ca^{2+} pathway. Again, WNT5A binds to the Ror1/2 and Fz receptors leading to phosphorylation of Dvl. In this pathway, Dvl leads to an increase in intracellular Ca^{2+}. Ca^{2+} acts as a second messenger that leads to activation of protein kinase C (PKC) and calmodulin-dependent protein kinase II (CamKII). CamKII blocks beta-catenin signaling by inhibiting the beta-catenin-Tcf/Lef transcription factors bound to gene promoters (Kikuchi et al., 2012). Activation of CamKII and PKC also leads to changes in cell migration and invasion (Nishita et al., 2010; Figure 1).

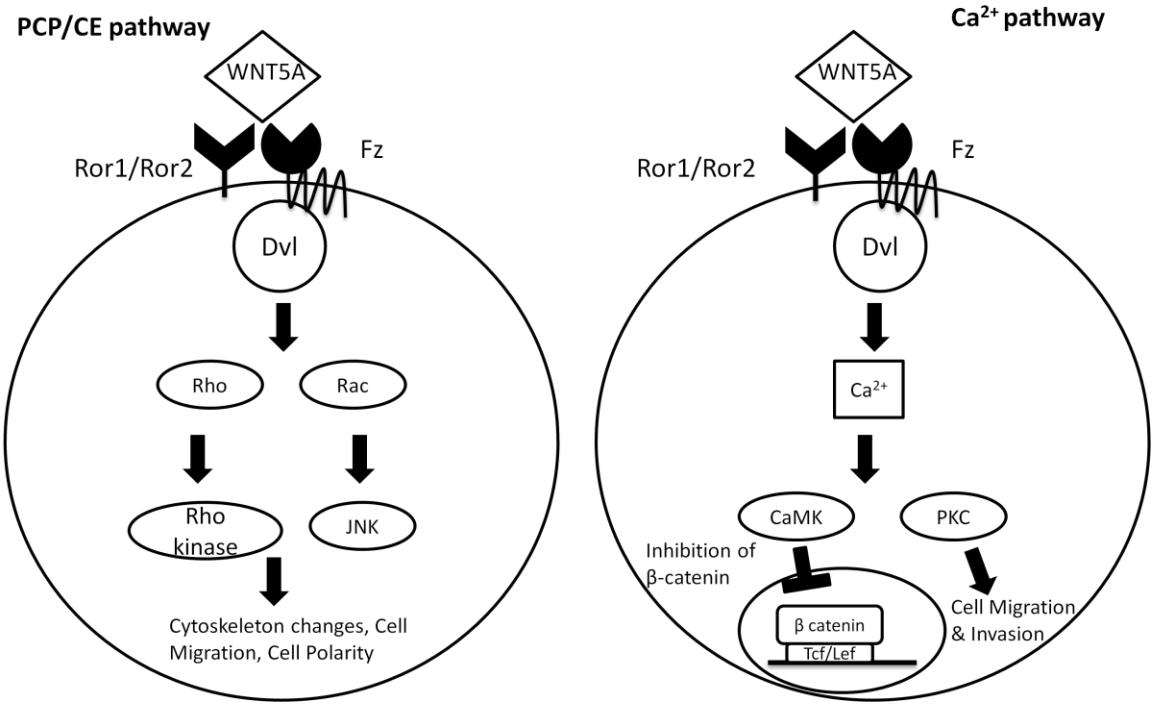

Figure 1. WNT5A Signaling Pathways. WNT5A signals through the beta-catenin independent pathways. **A**. The planar cell polarity (PCP)/convergent extension (CE) pathway. WNT5A signaling cascades through this pathway to effect cytoskeletal changes, cell migrations and cell polarity. **B**. The Calcium (Ca^{2+}) pathway. WNT5A signals through this pathway to inhibit to inhibit beta-catenin and gene expression. This leads to cell migrations and invasion. CaMK, Ca^{2+}/calmodulin-dependent kinase; Dvl, disheveled; Fz, Frizzle; PKC, protein kinase C; JNK, c-Jun N-terminal kinase; Tcf/Lef, T-cell factor/lymphoid enhancer factor. Based on diagrams in Kikuchi et al. (2012) and Nishita et al. (2010).

More relevant to this proposal is the signaling interaction between WNT5A and osteoblasts.WNT5A activates the non-canonical pathways that can interfere with the canonical Wnt signaling in osteoblasts.WNT5A is expressed in osteoblast stem cells and Ror2 is expressed in precursor osteoclasts. Mice deficient in WNT5A and Ror2 display disruptions in osteoclast production. These results suggest WNT5A is crucial for osteoclast generation and osteoclast homeostasis (Maeda et al., 2012).

Cellular Functions of WNT5A

WNT5A signaling is required in various cell functions related to cell movement, including cell adhesion and cytoskeletal rearrangement.WNT5A signaling regulates cell adhesion by activating G proteins and other kinases in the cell (See Figure 1). WNT5A activates the G protein Rac, which is responsible for regulating the lamellipodium of migrating cells. Focal adhesion kinase (FAK) is also regulated by WNT5A. FAK is involved in adhesion turnover by controlling microtubule polarization (Kikuchi et al., 2012; Mitra et al., 2005). In one study, WNT5A knockdown disrupted cell adhesion, cell migration and FAK (Matsumoto et al. 2010).

In embryonic fibroblasts, WNT5A induces cell migration via Ror 2. It is proposed that the formation of lamellipodium in fibroblasts is mediated by Ror 2 and filamin A (FLNa), which is an actin-binding protein. In addition to the lamellipodium formation, WNT5A mediates the reorganization of the microtubule organizing center, which includes the involvement of Ror 2, FLNa and JNK. APC also functions as a microtubule-plus-end binding protein that is boosted by WNT5A signaling. Dvl and the APC complex bind FAK and paxillin, a focal adhesion molecule. FAK and paxillin are responsible for microtubule stabilization around the cell's leading edge, which is important for cell migration (Wong et al., 2003).

WNT5A is also involved in mesenchymal cell differentiation. Chondrocytes and osteoblasts share common precursor mesenchymal stem cell. WNT5A-deficient mice, either die prematurely around childbirth or the mice have truncated limbs and proximal

skeletons (Yamaguchi et al., 1999). The researchers of this study determined that the death and abnormally shortened limbs were due to a significant decrease in cell proliferation. This decrease was due to the absence of WNT5A recruiting mesenchymal stem cells, reduced induction of chondrocyte proliferation, and deregulation of hypertrophic stages (Yamaguchi et al., 1999; Yang et al., 2009). It is speculated that WNT5A inhibits the beta-catenin pathway in the stem cells to decrease osteogenesis and promote chondrogenesis (Bradley and Drissi, 2010).

WNT5A Gene Structure and Protein Isoforms

The human *WNT5A* gene is located on Chromosome 3, band p14, between 55,499,744 and 55,521,331 base pairs. The human *WNT5A* gene has different transcription start sites and alternative splicing that generates six transcripts (Ensembl, EN5600000114251). These transcripts give rise to four proteins (Table 1). The transcript, WNT5A-201 (ENST00000264634) is 5837 base pairs long with 5 exons and 4 introns that encodes a protein of 380 amino acids (Figure 2). This transcript is derived from what is referred to in the lab as Promoter A (Katula et al., 2012) and is the most studied of the *WNT5A* transcripts. It corresponds to the cDNA RefSeq NM_003392. Another transcript, WNT5A-005, is produced from the transcription start site referred to as promoter B, within the first intron of the Promoter A transcription unit (Figure 2). The Promoter B transcript encodes a protein of 365 amino acids and is 15 amino acids shorter than the derived Promoter A protein. The Promoter A transcript has a unique Exon 1, whereas the Promoter B transcript includes a unique Exon 1β (Figure 2). Exons 2, 3, 4 and 5 are

common to both transcripts (Bauer et al., 2013). The unique Exon 1 and Exon 1β sequences were used to develop Taqman primer-probes specific to Promoter A and Promoter B transcripts, respectively (Katula et al., 2012).

Table 1. Human WNT5A Gene Transcripts and Proteins [1]

Name	Length (basepair)	Length (amino acids)	Biotype
WNT5A-001	6042	380	Protein coding
WNT5A-201	5837	380	Protein coding
WNT5A-005	5576	365	Protein coding
WNT5A- 009	959	214	Protein coding
WNT5A-007	521	-	Processed transcript
WNT5A-008	661	-	Retained intron

[1] Derived from Ensembl ENST00000264634. The length of the WNT5A-005 transcript was updated based on Bauer et al. (2013)

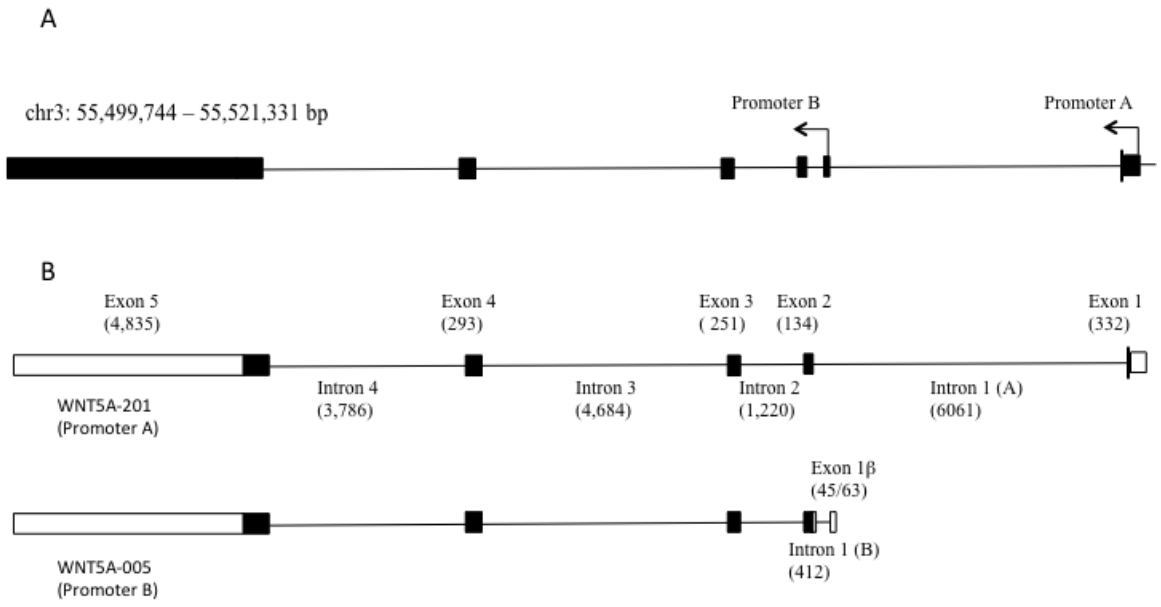

Figure 2. *WNT5A* Gene Transcripts. A. The location of Promoter A and Promoter B transcription start sites and exons on Chromosome 3. **B.** Promoter A and Promoter B primary transcripts. Black boxes are coding regions; open boxes are untranslated regions. Sizes in nucleotides of the exons and introns are shown in parenthesis. Exon 1 is unique to Promoter A; Exon 1β is unique to Promoter B. This diagram is based on the Ensembl EN5600000114251 and Bauer et. al, 2013.

Until recently, WNT5A studies have focused on the Promoter A transcript and its derived protein. In a recent study, Bauer et al. (2013) provide evidence that the protein isoforms from transcripts Promoter A and Promoter B are functionally distinct. They showed that after processing in the rough endoplasmic reticulum, the Promoter A derived protein (termed isoform WNT5A-L) has an additional 18 N-terminal amino acids compared to the Promoter B derived protein (termed isoform WNT5A-S). Functional analyses indicate that in some cancers, isoform WNT5A-L reduces proliferation, whereas isoform WNT5A-S increase cell proliferation. This suggests that differential expression of the isoforms could affect cell proliferation. There was no distinction observed between

the isoforms with regards to their effects on the beta-catenin Wnt signaling pathway; both inhibit the pathway to the same degree.

WNT5A and Cancer

WNT5A levels have been shown to vary in a wide range of cancers such as lung, gastric, pancreatic, prostate, osteosarcoma (Huang et al., 2010; Kurayoshi et al., 2006; Ripka et al., 2007; Wang et al., 2010; Enomoto et al., 2009). It appears, however, that WNT5A can function in some cancers as an oncogene and in others as a tumor suppressor. This is supported primarily by the finding that WNT5A can be overexpressed or inactivated, depending on the cancer type. There is also some experimental evidence that WNT5A has tumor suppressor or oncogenic functions, based primarily on overexpression of WNT5A from transfection of expression vectors and siRNA knockout studies.

Most significantly, high levels of WNT5A expression have been associated with metastasizing cancers. WNT5A protein was found to be highly expressed in the leading edge of cells in non-melanoma skin cancer (Pourreyron et al., 2012). High levels of WNT5A gene expression was detected in invasive pancreatic adenocarcinomas (Bo et al., 2013). Experimentally, transfection of a WNT5A expression vector lead to increased melanoma cell invasion associated with protein kinase C (PKC) activation and increased cell invasion (Weeraratna et al., 2002). In osteosarcoma, WNT5A expression promotes invasiveness and migrations. In the cell lines, SaOS-2 and U20S, constitutively active WNT5A and Ror2 were found to increase actin protrusions, invadopodias and

degeneration of the extracellular matrix that is mediated by MMP-13 (Enomoto et al., 2009). In another study,WNT5A overexpression caused constitutive activation of WNT5A-Ror 2 signaling that lead to expression of matrix metalloproteinase (MMP) that leads to invasiveness of prostate cancer cells (Yamamoto et al., 2010). Zhang et al. (2014) found that WNT5A promotes migration of human osteosarcoma cells through the phosphatidylinositol-3 kinase/Akt signaling pathway.

Most WNT5A studies have focused on the Promoter A transcript and protein isoform. Our lab and Bauer et al. (2013) provide evidence that WNT5A Promoters A and B are differentially regulated in cancer. Bauer et al. (2013) showed that the WNT5A-L transcript (Promoter A) is down regulated, whereas the WNT5A-S transcript (Promoter B) is overexpressed in HeLa (cervical), MDA-MB-231 (breast) and SA-SY5Y (neuroblastoma) cancer cell lines. These results suggest that WNT5A-S (Promoter B) is functioning as an oncogene, whereas WNT5A-L (Promoter A) is a tumor suppressor. Contrary to Bauer et al. (2014), we found that *WNT5A* Promoter B transcripts are nearly absent in the osteosarcoma cell line, SaOS-2 (Hsu, 2012), whereas, Promoter A is active. Normal osteoblasts were found to produce both transcripts, with Promoter B transcripts at a higher level (Hsu, 2012). This suggests that during osteoblast transformation, Promoter B is being silenced, indicating it may have tumor suppressor function.

WNT5A Epigenetic Regulation

WNT5A misregulation in cancer appears to be due to nongenetic or epigenetic changes rather than gene mutation. Epigenetic changes include DNA methylation and

histone modifications. DNA methylation involves the addition of a methyl group to the 5 carbon position on cytosine, usually to CpG dinucleotides, by DNA methyltransferases (dnmts). Different DNA methyltransferases are responsible for initiation and maintenance of methylated DNA. Normal patterns of genomic DNA methylation are established in during early embryogenesis, where nearly all CpGs are methylated. CpG are commonly found around promoter regions of genes where DNA methylation is usually associated with transcriptional repression.

WNT5A methylation has been detected in cancer types in which the gene is not expressed. In one study, six different colorectal cancer cell lines were tested for their level of *WNT5A* methylation (Ying et al., 2008). In the cell lines with low levels of *WNT5A* expression, they showed total methylation of the *WNT5A* gene. One cell line with moderate levels of *WNT5A* expression showed weak methylation of *WNT5A*. The sixth cell line with a high amount of *WNT5A* had no methylation. Also, WNT5A expression could be induced by knockout of two dnmts. These results indicate that the *WNT5A* promoter (A) region is methylated in colorectal tumors to reduce its activity and that *WNT5A* methylation is mediated by dnmts (Ying et al., 2008)(Ying et al., 2008).

In leukemia, *WNT5A* was also shown to be methylated (Martín et al., 2010). In a study on acute myeloid leukemia (AML), they assessed the difference in *WNT5A* expression in seven AML cell lines and bone marrow cells from healthy donors. They found that the *WNT5A* promoter region was methylated in low *WNT5A* expressing AML cell lines and completely unmethylated in healthy bone marrow tissue. These findings

indicate that *WNT5A* expression is modified by DNA methylation during leukemia tumorigenesis. It is important to note that the Promoter A genomic region was analyzed in these studies.

Methylation analysis of Promoter B associated CpG's in osteoblasts and SaOS-2 osteosarcoma cells was conducted in our lab (Vaidya, 2013). In normal osteoblasts, six identified CpG islands were found to be completely unmethylated. In the SaOS-2 cell line, the six different CpG islands show different levels of methylation. The most 5' CpG islands nearest to Promoter A, 1 and 2, were totally unmethylated. CpG islands 3, 4, and 5 were completely methylated. CpG island 6, which includes the Promoter B transcriptional start site and Exon 1β sequences, showed partial methylation with the first fifteen CpGs unmethylated and the last eleven CpG methylated. Treatment of SaOS-2 cells with 1 μM 5-aza-2'deoxycytidine for 72 hours lead to reactivation of Promoter B and a slight reduction in methylation in CpG island 6 (Vaidya, 2013). Together, these results support the conclusion that the *WNT5A* Promoter B is inactivated in SaOS-2 cells due to DNA methylation.

It is likely that histone modifications plays a role in the epigenetic regulation of WNT5A expression in cancer cells. Histones are proteins involved in packaging DNA into chromatin structures within the nucleus, which can be modified to control gene expression. Two each of the four histones, H2a, H2b, H3, H4 associate to form a core around 147 base pairs of DNA wraps to form a nucleosome. Modifications of histones take place at the amino acid residues on the histone N-terminal tail. Histone

modifications alter gene expression by affecting nucleosome structure, which allows for repression or expression of a gene. The focus of this research project is the histone modification, methylation. Most histone methylation occurs on the lysine and arginine amino acids on the histone tail. Methylation can inhibit or activate gene expression depending on the location of the amino acid methylation and how many times that amino acid is methylated. For example, H3K27me3 (trimethylated on lysine residue 27) is a repressive histone mark, whereas H3K4me3 is an activating histone mark (Ekström et al., 2009).

DNA methylation and histone modifications have a relationship in regulating gene expression. As such, any observed change in DNA methylation would be expected to alter histone modifications. In early development, it has been proposed that histone modifications are implemented before *de novo* methylation. Following fertilization, CpG's become unmethylated across the genome except for imprinted regions. Before *de novo* methylation, histone H3 is methylated at active gene regions to H3K4me. At the time of *de novo* methylation when the embryo implants, the DNA methyltransferases Dnmt3 cannot methylate regions that have the H3K4me (Guenther et al., 2007). This explains the correlation between the presence of an active histone marker and no DNA methylation. DNA methylation is important for maintaining histone modifications after DNA replication (Bostick et al., 2007). Chromatin structures are disrupted when the replication fork progresses along DNA, after which the DNA methylation pattern is used as a marker to reconstruct the histone modifications (Cedar and Bergman, 2009).

Histone modifications have been associated with silencing of *WNT5A* in certain colon cancer cell lines. In this study both a metastatic, SW620, and non-metastatic, SW480, colon cancer cell lines were tested for epigenetic alterations (Li & Chen, 2012). The cell lines were treated with 5-aza-cytidine but neither cell line showed any change. This suggested that WNT5A expression was not caused by the DNA methylation. The SW620 cells were treated with the histone deacetylase inhibitors, trichostatin A and sodium butyrate, which lead to an increase in WNT5A expression. ChIP was also to detect histone modifications before and after treatment with sodium butyrate. Low levels of H3Ac, H4Ac, and H3K4me2 were found in SW620 while high levels of H3K27me3 were found in SW620 in comparison to SW480. After treatment with sodium butyrate, H3Ac was increased at the promoter regions in both cell lines. H3K4me2 was higher at the coding and promoter regions of SW620.

Considering that increased DNA methylation has been detected in the *WNT5A* Promoter A and B genomic regions in different cancer types, it would be expected that histone modifications will be associated with these changes and the silencing of Promoter B in the SaOS-2 cell line. The goals of this study are to determine if lack of Promoter B expression and increased DNA methylation at specific sequence regions and if specific modified histones are more enriched at Promoter A or B. To accomplish these goals the following specific aims were completed:

1. Determined the level of the *WNT5A* Promoter A and Promoter B transcripts in human osteosarcoma primary tumor tissue and U20S cell line.

2. Determined the DNA methylation profiles in *WNT5A* intron 1 CpG islands of the osteosarcoma cell line U20S.
3. Compared the histone modifications in WNT5A intron 1 at select CpG islands of the osteosarcoma cell lines SaOS-2 and U20S.

CHAPTER II

MATERIALS AND METHODS

Cell Culture

U20S (HTB-96) and SaOS-2 (HTB-85) osteosarcoma cells were obtained from the American Type Culture Collection (ATCC). The SaOS-2 cells were grown in McCoy's 5a Modified medium containing 15% fetal bovine serum and penicillin/streptomycin (50 I.U. /50 µg per ml) (referred to as 15% Complete McCoy's 5a). The U20S cells were grown in 10% fetal bovine serum and penicillin/streptomycin (50 I.U. /50 µg per ml) (referred to as 10% Complete McCoy's 5a). The U20S and SaOS-2 cells were grown at 37°C in a 5% CO_2 humidified cell culture incubator.

Quantitative Real Time-PCR (qRT)-PCR

RNA Isolation

The medium was removed from the U20S cells grown in 100 mm plates. The cells were washed with cold 1x Phosphate Buffered Saline (PBS) and 5 ml of cold 1x PBS was added to the plates. The cells were scraped from the plates and transferred to a 15 ml Falcon tube. The cells were centrifuged for 5 minutes at the #4 setting in a clinical

centrifuge and the supernatant was removed. RNA was isolated from the cell pellet using the SV Total RNA Isolation System (Promega, Z3105). 175 µl of RNA Lysis Buffer was added to the pelleted cells. The cell lysate was sheared using a 20-gauge needle, 4-5 times to shear the genomic DNA. 350 µl of RNA Dilution Buffer was added. The sample was mixed and heated at 70 °C for three minutes. The sample was centrifuged for 10 minutes at 14,000 rpm and the cleared lysate was transferred to a new microcentrifuge tube. 200 µl of 95% ethanol was added to the cleared lysate and mixed. The sample mixture was added to a Promega RNA isolation column and spun at top speed in a microcentrifuge for 1 minute. The column was washed with 600 µl RNA Wash Solution. The column was centrifuged for 1 minute. 50 µl of DNase incubation mix (containing 40 µl of Yellow Core Buffer, 5 µl 0.9M $MnCl_2$ and 5 µl of DNase I enzyme) was applied to the membrane of the column and incubated for 15 minutes at room temperature. After incubation, 200 µl of DNase Stop Solution was applied to the column and the column was centrifuged for 1 minute. The column was washed with 600 µl RNA Wash Solution and centrifuged for 1 minute. The sample was washed again with 250 µl of RNA Wash Solution and centrifuged for 2 minutes. The RNA was eluted from the column with 100 µl of nuclease free water and centrifuged for 1 minute. The purity and quantity of the U20S RNA was determined by reading at 260 and 280 nm.

5 µg of derived RNA from three primary human osteosarcoma tissues was obtained from Origene Technologies. Patient 1 RNA (CR559626) was isolated from a humerus parosteal osteosarcoma. Patient 2 RNA (CR562179) was isolated from

metastatic osteosarcoma. Patient 3 RNA (CR560767) was isolated from a recurrent osteosarcoma.

cDNA Synthesis

The U20S RNA and the RNA from the three primary osteosarcoma tumor tissues were converted into cDNA using the QuantiTect Reverse Transcription Kit (Qiagen, 205313). A 1x reaction mixture consisted of 1µg of RNA, reverse transcriptase, reverse transcriptase buffer, primers, gDNA, and nuclease free water to give a final 20 µl reaction. The reverse transcriptase sample mixture was incubated for 5 minutes at 42 °C and then incubated at 95 °C for 3 minutes.

The resulting cDNA was then used in qRT-PCR reaction to quantify Promoter A and Promoter B transcripts. Each reaction was run in triplicate with three target primer-probes; Promoter A, Promoter B, and Glyceraldehyde 3-phosphate dehydrogenase (GAPDH) (internal control) (Applied Biosystems HS99999905_m1) for each cDNA sample (U20S and three primary tumor tissues). Also, quantified Promoter A and Promoter B PCR products were run in triplicate to generate a standard curve. Standard curves were used to quantify the exact amount of Promoter A and Promoter B transcript levels. Using the line equation of the standard curves, the transcript levels of Promoter A and Promoter B can be calculated from the C_t values of the samples. The sequence of Promoter A and Promoter B primer-probes are given in Table 2.

Table 2. Taqman Primer-Probes for WNT5A Promoter A and Promoter B

	Sequence (5' → 3')	Length (base)	Product Size (bp)
Human Promoter A			
Forward	TCGGGTGGCGACTTCCT	17	77
Reverse	CGCCCCCTCCCCCTCGCCATGAAG	24	
Probe	TAACCTTATAATTCGGGTCCTCAAC	25	
Human Promoter B			
Forward	CCTCTCGCCCATGGAATT	18	71
Reverse	CTTCAGGTAACCTTATAATTCGGG	24	
Probe	CTGGCTCCACTTGTTGCTCGGCC	23	

(Hsu, 2011)

Bisulfite Sequencing

Genomic DNA Isolation

U20S cells were plated in 100 mm plates and grown for 2-3 days. The medium was removed and the cells were washed with 5 ml of 1x Hank's. The cells were trypsinized and 3 ml of 10% Complete McCoy's 5a medium added. The cells were transferred to a 15 ml Falcon tube and pelleted. The pelleted cells were resuspended in 3 ml of 1x PBS and counted using a hemocytometer. Aliquots representing $1x10^5$ were transferred to a microcentrifuge tube and pelleted. Genomic DNA was isolated from the cells following the directions of the Genomic DNA Isolation kit (Zymo research, D3004). To the pelleted cells, 10 µl of Zymobeads and 200 µl of Genomic Lysis Buffer were added and mixed. The sample stood at room temperature for 2 minutes and was centrifuged at 5,000 rpm for 1 minute. An additional 250 µl of Genomic Lysis Buffer was added to the sample and mixed. The sample was centrifuged for 1 minute at 5,000 rpm.

The sample was resuspended in 500 µl of gDNA Wash Buffer and centrifuged for 1 minute at 5,000 rpm. Additionally, 500 µl of gDNA Wash Buffer was added to resuspend the sample pellet. The sample was centrifuged for 1 minute at 5,000 rpm. After the washes, 35 µl of Elution Buffer was added to the sample. The sample pellet was vortexed to break up the pellet and then incubated at 65°C for 5 minutes. The sample was vortexed briefly and centrifuged at maximum speed for 1 minute. The supernatant containing the genomic DNA was collected. The U20S genomic DNA quantity and purity was determined by reading an aliquot at 260 to 280 nm.

Bisulfite Conversion

The U20S genomic DNA was bisulfite converted using the EZ DNA Methylation-Direct Kit (Zymo Research, D5020). 500- 550 µg of genomic DNA was added to 5 µl of Dilution Buffer and adjusted to 50 µl using nuclease free water. The DNA mixture was incubated at 37°C for 15 minutes and the 100 µl of CT Conversion Reagent was added to the DNA sample mix. The sample mix incubated in the dark for 12-16 hours at 50°C. The sample mix was incubated on ice for 10 minutes. On a Zymo-Spin™ IC Column, 400 µl of Binding buffer and sample was loaded. The buffer and sample mix were mixed and centrifuged at maximum speed for 30 seconds. The column was washed with 100 µl Wash Buffer and centrifuge at maximum speed for 30 seconds. After centrifugation, 200 µl of Desulphonation Buffer was added to the column and incubated at room temperature for 20 minutes. The column mix was centrifuged at maximum speed for 30 seconds. The column was washed twice with 200 µl of Wash Buffer and centrifuged at maximum

speed for 30 seconds. In a new microcentrifuge tube, the bisulfite converted DNA was eluted using 10 µl of Elution Buffer. The bisulfite converted DNA was read at 260 nm to 280 nm to determine purity and quantity.

PCR Amplification and Subcloning

1 µl of bisulfite converted DNA was used in PCR amplification using the previously designed WNT5A CpG Island primers specific for converted DNA of each of the six regions (Vaidya, 2013). The PCR amplification used the ZymoTaq DNA polymerase (Zymoresearch, E2001) at the appropriate amplification conditions listed in Table 3. The PCR product was verified by running 10 µl of the PCR products on a 2% agarose gel with 100 base pair marker and visualized through UV transillumination.

Verified PCR products were extracted and purified using the QIAquick Gel Extraction Kit (Qiagen, 28704). The remaining 40 µl of PCR product were run on a 2% low melt agarose gel using 100 base pair marker and visualized through UV transillumination. The correct DNA band was excised from the agarose gel and placed in a microcentrifuge tube. The gel slice was weighed and 3 volumes of QG Buffer was added to the gel slice. The gel slice was incubated at 50°C for 10 minutes or until the gel was dissolved. A gel volume of isopropanol was added to the dissolved gel and mixed. The sample was applied to a QIAquick Spin Column and centrifuged for 1 minute. The column was washed with 750 µl of PE Buffer and centrifuged for 1 minute. The purified DNA was eluted from the column using 50 µl of Elution Buffer. The purified DNA was read at 260 and 280 nm for purity and quantity.

The purified DNA was cloned in the pGEM-T vector using the pGEM-T Easy Vector System (Promega, A1360). The amount of purified DNA cloned into the vector was calculated based on base pair size of the insert using the formula provided. The ligation reaction was incubated overnight at 4°C. After ligation, 5 µl of the ligation reaction was transformed into 100 µl of competent DH5α *E.coli*. The competent cells plus ligation mix was incubated on ice for 20 minutes. The cells were heat shocked for 45-50 seconds at 42°C. The tubes were returned to ice and 500 µl of room temperature SOC medium was added. The cells were incubated with shaking for 1 hour at 37°C. 200 µl of the cells were plated onto Luria Broth (LB) – Ampicillin (AMP) plates with 40 µl X- gal (5-bromo-4-chloro-3-indolyl-beta-D-galacto-pyranoside) (40 mg/ml) and incubated overnight at 37°C.

Table 3. Bisulfite Sequencing PCR Primers, Anneal Temperature and Product Size

Primer Name	Sequence (5'-3')	Anneal Temp	Size (bp)
W5AR1F	AGTAATAGGATAATGATTTAATTTAATAAA	45°C	393
W5AR1R	CAAAATACCTAAACTCACCCAATA		
W5AR2F	AGTTTTTAGATAGATTTTGTTAGGGGAGT	45°C	255
W5AR2R	CATAATACTAACCCCTTAAACACC		
W5APrBR2HF	GTTTAAGAGTTTTTTGTTTTTTTT		335
W5APrBR2HR	AAATACCAACCCTATATCCAACTAAC		
W5aR3F#2	GAGGATTTTTGTTTGGTTTTTTTATT	55°C	441
W5AR3R	AAACTAAATATTTTCCAACACTTTC		
W5AR4F	GTTTTGGGAATTGGTGGATTT	45°C	329
W5AR4R	AACCCAAACTACAAAATCAACTCTC		
W5AR4F3H2	GAATTTGTTATTAATTTTTTTGTTGTTTG	58°C	226
W5AR4R3H2	TACAAAATCAACTCTCCCCAAAA		
W5APrBR5nF	AGGGTTGTTTAGGTTTTTTTTGTTT	45°C	578
W5APrBR5nR	AACTCCAATTTCCCTTAATCCTAAT		
W5AR6F	TTTTTTTTAGTTTGGTTGAAGAA	55°C	393
W5AR6R	CCTAAATAATTCACTCAAAAACCC		
W5AR6H2F5	AATTAATTTTGGTTTTATTTGTTGTT	55°C	96
W5AR6H2R5	TCAATCCCTCCTAAATAATTCACTC		

(Vaidya, 2013)

Plasmid Screening, Plasmid Purification and Sequencing

White colonies grown on a LB-AMP master plate and cultured overnight at 37°C in 3 ml of LB containing 100 µg/ml ampicillin were picked. The overnight culture was used to conduct a quick miniprep analysis method using a boiling water bath (Riggs and McLachlan, 1986). 1 ml of the cultured broth was centrifuged for 1 minute at maximum speed. The supernatant was removed and the bacteria pellet resuspended in 200 µl of Lysis Buffer/Lysozyme mixture (8% sucrose, 0.5% triton X-100, 50 mM EDTA, 10 mM Tris-HCl (pH 8.0) with 750 µg lysozyme per ml). The samples were boiled for 40 seconds then immediately placed on ice. The sample was centrifuged for 10 minutes at maximum speed and placed on ice. 10 µl of the supernatant was removed and run on a 2% agarose gel with Lambda phage Hind III marker. The gel was visualized through UV transillumination and photographed using a Bio Rad Molecular Imager Gel Doc XR system. Samples showing a supercoiled plasmid band running slower than the plasmid band in the "without insert" blue control sample were further purified for sequencing using the Qiagen QIAprep Miniprep kit (Qiagen, 27106). The remaining 2 ml of the liquid culture was centrifuged for 5 minutes and the supernatant removed. The bacteria pellet was resuspended in 250 µl of P1 Buffer. Next, 250 µl of P2 Buffer was added and mixed thoroughly. 350 µl of N3 Buffer was added to the sample and the sample was mixed thoroughly. The sample was centrifuged for 10 minutes at 13,000 rpm. Supernatant from centrifugation was applied to a QIAprep Spin Column. The column was centrifuged for 1 minute. The column was washed with 750 µl of PE Buffer and

centrifuged for 1 minute. The purified plasmids were eluted by adding 50 µl of Elution Buffer to the column and letting it sit for 1 minute before centrifuging for 1 minute. 10 µl of the purified plasmids of at least 100 ng/ul were sent to Eurofin MWG Operon sequencing facility for sequencing. The plasmid DNA concentration was determined by reading the OD at 260 to 280 nm. Plasmid samples that were too dilute were concentrated in a speed vac concentrator.

DNA Sequencing Analysis

DNA Sequencing was performed by Eurofin MWG Operon. Using the MacVector Sequence (Version 12.0.3) analysis software, each sequence was aligned to a computer generates bisulfite converted sequence of that region assuming all C's are methylated. As such all C's in the CpG island remain a C and all other C's were converted to T's. Once aligned, an unmethylated experimental CpG would be converted to a T and would not align the methylated CpG, which remains a C. A methylated experimental CpG would remain a C and would align the methylated CpG.

Chromatin Immunoprecipitation (ChIP) Assay

Cell Fixation

A ChIP assay was performed following the instructions of the ChIP –IT Express kit (Active Motif, 53008) to study the histone modifications in U20S and SaOS-2 cell lines. The U20S and SaOS-2 cells were grown to 70% confluency using nine 100 mm plates for each cell line. The medium was poured off the plates. The cells were fixed by

adding 6.5 ml of 37% Formaldehyde Fixation Solution per plate and shaking for 10 minutes at room temperature. The Fixation Solution was poured off and the plates were washed with 3.3 ml cold 1x PBS. The PBS was poured off and 3.3 ml Glycine Stop Solution was added to the plates and incubated at room temperature with shaking for 5 minutes. The Glycine Stop solution was removed and the cells were washed with 3.3 ml cold 1x PBS. 1.5 ml of Cell Scraping Solution (containing 120 µl of phenylmethanesulfonyl fluoride (PMSF) (100mM) was added to each plate and the cells were scraped then transferred to a 15 ml Falcon tube. The cells were pelleted by centrifuging at 4°C for 10 minutes at 2,500 rpm. The supernatant was removed and chromatin shearing was immediately conducted. We determined that the fixed cells could not be frozen before chromatin shearing.

Chromatin Shearing

The pelleted cells were resuspended in 3 ml of ice cold Lysis Buffer [supplemented with 15 µl of Protease Inhibitor Cocktail (PIC) and 15 µl of PMSF (100mM)] and incubated for 30 minutes on ice. The cells were transferred to an ice cold Dounce homogenizer and dounced on ice with about 30 strokes to help with nuclei release. Looking at dounced cells under a phase contrast microscope was helpful to ensuring nuclei release. The dounced cells were transferred to a 1.5 microcentrifuge tubes and centrifuged for 10 minutes at 5,000 rpm at 4°C to pellet nuclei. The supernatant was removed and the nuclei resuspended in 300 µl of Shearing Buffer [supplemented with 5 µl PIC and 5 µl of PMSF (100 mM)]. The samples were placed on ice and different

sonication conditions were tested. The best sonication conditions for U20S was 10 pulses of 20 seconds on and 40 Seconds off between level 1 and 2 on a 60 Sonic Dismembrator. The best sonication conditions for SaOS-2 was 12 pulses of 20 seconds on and 40 seconds off between level 1-2 on a 60 Sonic Dismembrator (Fisher Scientific). The sheared chromatin was centrifuged for 10 minutes at 14,000 rpm at 4°C. The supernatant containing the sheared chromatin was transferred to new microcentrifuge tubes. 50 µl aliquots from each chromatin sample were put into new microcentrifuge tubes for analysis of DNA size.

DNA Clean Up and Shearing Efficiency Test

To the 50 µl aliquots of each sample, 150 µl of deionized water and 10 µl of 5M NaCl were added. The samples were heated to 65°C in a thermocycler overnight to reverse cross link the fixed chromatin sample. 1 µl of RNase A (10 µg/µl) was added to each sample which were incubated at 37°C for 15 minutes. Next, 10 µl of Proteinase K (0.5 µg/µl) was added to each sample and incubated at 42°C for 90 minutes. Then, 200 µl of 1:1 phenol/chloroform TE saturated pH 8.0 was added to the samples, mixed and centrifuged for 5 minutes at maximum speed. The aqueous phase was transferred to a new microcentrifuge tube. To the aqueous phase, 20 µl of 3M sodium acetate, pH5.2 and 500 µl 100% ethanol was added and mixed completely. The samples were placed at -80°C for 1 hour. The samples were centrifuged at maximum speed for 10 minutes at 4°C. The supernatant was removed and without disturbing the pellet, 500 µl of ice cold ethanol was added. The samples were centrifuged at maximum speed for 5 minutes at 4°C. The

supernatant was removed and the pellet air dried. The dried pellet was resuspended in 30 µl of sterile water. The concentration and purity of the DNA was measured at 260 and 280 nm. On a 1% agarose gel, 5 µl of the DNA samples were run with 100 base pair marker, and visualized by UV transillumination, and photographed. Sheared chromatin showing DNA between 200-1500 base pair were used for immunoprecipitation.

Immunoprecipitation

The sheared chromatin with the correct DNA size spread was used in immunoprecipitation. In a new microcentrifuge tube, 10 µl of this sheared chromatin was extracted as "Input DNA" to be used later in PCR analysis. Using the provided siliconized 1.7 ml microcentrifuge tubes, a 100 µl reaction mix was made using 25 µl Protein G Magnetic Beads, 10 µl ChIP Buffer 1, 25 µg of sheared chromatin, 1 µl PIC, water, and 1-3 µg of antibody. (Antibody was added last to the reaction.) Antibodies for the different samples were RNA Polymerase II (Active Motif 39097), IgG and H3K27me3 (AbCam ab6002). A bridging antibody was used with the RNA polymerase II, mouse monoclonal anti-H3K27me3 and IgG (Active Motif 53017). The samples were incubated on a rotator overnight at 4°C. After incubation, the samples were centrifuged briefly and placed on the magnetic stand to pellet the beads to one side of the tube. The supernatant was removed and 800 µl of ChIP Buffer 1 was used to resuspend the beads. The beads were pelleted again using the magnetic stand. Then, 800 µl of the ChIP Buffer 2 was added twice to resuspend the pelleted beads. The Wash Buffer was removed completely.

Elution of Chromatin, Reverse Cross Linking and Proteinase K Treatment

The beads were resuspended in 50 µl of Elution Buffer AM2. The beads and buffer were incubated at room temperature for 15 minutes on a end to end rotator at 4°C. Tubes were briefly centrifuged and 50 µl of Reverse Cross Linking Buffer was added. The samples were mixed by pipetting and the tubes were placed on the magnetic stand. The supernatant containing the chromatin was transferred to a thermocycler tube. The "Input DNA" was processed by adding 88 µl of ChIP Buffer 2 and 2 µl of 5M NaCl to the DNA. The ChIP samples and "Input DNA" was incubated at 95°C for 15 minutes in a thermocycler. The tubes were briefly centrifuged and 2 µl of Proteinase K (0.5 µg/µl) was added to each sample. The samples were mixed and incubated at 37°C for 1 hour. The Proteinase K Stop Solution was placed at room temperature during this incubation. After incubation, 2 µl of Proteinase K Stop Solution was added to the samples. The samples were centrifuged to collect the liquid.

Chromatin IP DNA Purification

The chromatin was purified using the Active Motif Chromatin IP DNA Purification Kit (Active Motif, 58002). For every volume of DNA sample, 5 volumes of DNA Purification Binding Buffer were added along with 5 µl of 3M sodium acetate. The samples were mixed and color of buffer was a bright yellow (If the color is bright orange or violet, additional 3M sodium acetate at 5 µl should be added until the color is yellow). The samples were applied to the DNA Purification columns and centrifuged at 14,000

rpm for 1 minute. To the column, 750 µl of Wash Buffer was added and centrifuged for 14,000 rpm for 1 minute. The uncapped tubes were centrifuged at 14,000 rpm for 2 minutes to remove residual Wash Buffer. The purified DNA was eluted by adding 50 µl of Elution Buffer to the column and centrifuging for 1 minute.

Primer Design

Due to the GC rich sequences of the WNT5A regions of interest, primers were designed visually. The primers were designed to be 16-25 base pairs, CG at the 3' end, melting temperatures within 3°C of each other and no more than 150 base pair amplicon length. The selected primers were analyzed for self-complementary and secondary structures using the Thermo Scientific Multiple Primer Analyzer (http://www.thermoscientificbio.com/webtools/multipleprimer/). The sequences of the ChIP primers are shown in Table 4. The primers for the Promoter B region flank Promoter B transcription start site, Exon 1β. The primers for Promoter A flank Promoter A transcription start site and the Exon1. The primers for Regions 3, 4 and 5 were outside of the targeted outside of the CpG island.

Table 4. ChIP qRT-PCR Primers

Primer name	Sequence(5'-3')
Promoter B	
2WntChipPrBExF2b	CCACCCCGCCTCCTTGG
2WntChipPrBExR2b	GCCACCCTCCGTCCTCTCC
WPrBChIPF2a	GCTCCACTCGCCTCCGTG
WPrBChIPR2a	GCCTCCTTCCTGCTCGCTC
Promoter A	
2WntProAChIPEx1F1	GCCTCTCCGTGGAACAGTTGC
2WntProAChIPEx1R2	CTGGGATGCGCCCAGG
WntProAEx1F4	CGCCAGTGCCCGCTTCAG
WntProAEx1R4	CAGCCGAGGAATCCGAGC
Regions	
ChipR3AFor	TGGGTCAAATGGGCTTCTTCC
ChipR3ARev	TCTGGGAGTGAAACGATGAGGG
ChipR4AFor	GAGATGCGACTCGTGAGGCTC
ChipR4ARev	GCTCCAGGGTAGAGGTAGGCAG
ChipR5AFor	GGCGGCTCACGGAGAAAAAC
ChipR5ARev	AAAAGGGGCAGAGGGGACC

Real Time PCR and Enrichment

ChIP enrichment was determined by qRT-PCR using SYBR-Green reagents. Each qRT-PCR set included a dilution series of the "Input DNA" to generate a standard curve for each primer set. The dilution series of the "Input DNA" consisted of three 10-fold dilutions of standard or 1, 1:10 and 1:100. The ChIP anti RNA polymerase II, IgG, anti- H3K27me3, anti-H3K9me3 and anti-H3K4me3 samples have different amplification profiles and were run in triplicate for each primer set. GAPDH was also used as a standard control for our ChIP samples and was run in triplicate with each primer set. GAPDH is a highly expressed gene. Using the linear regression plot of the "Input DNA", the Ct values of the different samples can be plotted and the enrichment

can then be calculated. The fold enrichment was determined according to the method for qRT-PCR described in ChIP-IT Express. The DNA quantity of the ChIP for a given primer and the negative control (IgG) were solved using the equation, $Y = M (\log X) + B$. Where X is the DNA quantity, Y is the cycle number for that sample, M is the slope of the standard curve, and B is the cycle number where X=1. The fold enrichment was calculated by the "ChIP DNA quantity" divided by "IgG DNA quantity".

CHAPTER III

RESULTS

WNT5A Promoter A and Promoter B Transcripts in Human Osteosarcoma Primary Tumor Tissue and U20S Cell Line

Higher Levels of Promoter A than Promoter B transcripts in U20S osteosarcoma cells

Previous results in the lab showed that *WNT5A* Promoter A transcripts are higher in comparison to Promoter B transcripts in the SaOS-2 osteosarcoma cell line, whereas in normal osteoblasts, Promoter B transcripts were higher than Promoter A transcripts (Hsu, 2012; Table 5). We wanted to determine if this pattern of *WNT5A* expression is specific to SaOS-2 or more general to osteosarcoma cells. RNA was isolated from the U20S osteosarcoma cell line and converted into cDNA. qRT-PCR was conducted using previously designed Taqman primer-probes that distinguish between Promoter A and Promoter B transcripts (Hsu, 2012). A five point standard curve was generated using purified PCR products with known molecule numbers for each dilution (Figure 3A). The standard curve line equation was used to calculate the copy numbers of the Promoter A and Promoter B transcripts per µg RNA using the generated C_t values of the samples (Figure 3B). This was repeated three times.

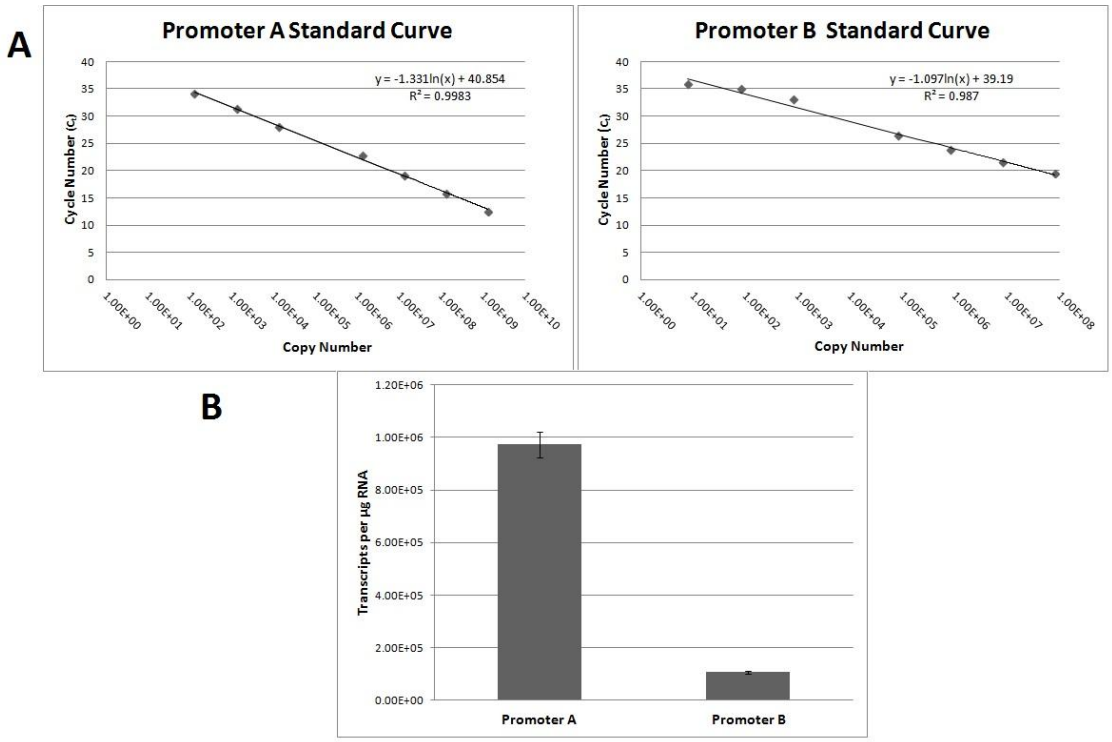

Figure 3. Promoter A and Promoter B Transcript Levels in U20S Osteosarcoma Cells. Total RNA was isolated from U20S, converted to cDNA, and used for qRT-PCR. **A**. Standard curves of Promoter A and Promoter B PCR products at known copy numbers. The derived linear equation for each line is shown. **B**. One example of quantification of Promoter A and B transcripts, expressed per µg RNA. The C_t values from qRT-PCR are used to solve for X in the linear equations of the standard curves. Bars are standard error calculated from three technical replicas.

There are higher numbers of Promoter A transcripts in comparison to Promoter B transcripts in the U20S cell line. From three independent determinations the average Promoter A to Promoter B transcript ratio was 11.9 (Table 5). These results confirm that Promoter A transcripts are higher than Promoter B transcripts in another osteosarcoma cell line (U20S) in addition to SaOS-2

. **Table 5.Transcript Numbers and Promoter A/Promoter B Ratio.**

Sample	Transcripts per µg RNA[1]	A/B Ratio
Normal osteoblast	A – $5.3 \times 10^6 \pm 0.8 \times 10^6$ B – $5.9 \times 10^7 \pm 1.6 \times 10^6$	0.09 ± 0.02[2]
Osteosarcoma cell line		
SaOS-2	A – $6.8 \times 10^6 \pm 0.5 \times 10^6$ B – $3.3 \times 10^4 \pm 0.7 \times 10^4$	224.5 ± 65.2[2]
U20S	A – $9.7 \times 10^5 \pm 1.5 \times 10^5$ B – $1.1 \times 10^5 \pm 0.7 \times 10^4$	11.9 ± 4.1
Osteosarcoma tumor tissue		
Patient 1	A – $5.3 \times 10^4 \pm 0.2 \times 10^4$ B – $6.3 \times 10^3 \pm 1.2 \times 10^3$	9.2 ± 3.5
Patient 2	A – $1.2 \times 10^5 \pm 0.03 \times 10^5$ B – $1.6 \times 10^4 \pm 0.05 \times 10^4$	7.5 ± 0.7
Patient 3	A – $7.9 \times 10^3 \pm 0.1 \times 10^3$ B – $1.1 \times 10^2 \pm 0.2 \times 10^2$	78.5 ± 27.8

[1] ±standard error, n=3. [2]Hsu, 2012. The p value for Promoter A to Promoter B transcripts for all samples was $P < 0.005$.

Osteosarcoma primary tumor tissues have reduced levels of Promoter B transcripts

Next we wanted to determine if the higher levels of Promoter A transcripts in comparison to Promoter B transcripts measured in both U20S and SaOS-2 was a characteristic of primary osteosarcoma tissue. The RNA from three different osteosarcoma patients was purchased. Patient 1 RNA was isolated from a humerus parosteal osteosarcoma. Patient 2 RNA was isolated from metastatic osteosarcoma. Patient 3 RNA was isolated from a recurrent osteosarcoma. Promoter A and Promoter B transcript copy numbers were quantified in these RNA samples by qRT-PCR using a standard curve, as described.

The results of one of the human primary patient tissue assays are shown in Figure 4. All three osteosarcoma tissue samples had higher Promoter A transcript levels in comparison to Promoter B. The A to B ratio for the three patient tissue samples are found in Table 5. Patient 1 and Patient 2 were more similar having 9.2x and 7.5x, respectively, more Promoter A than Promoter B transcripts, whereas Patient 3 had 78.5x more Promoter A than Promoter B transcripts. These results indicate that a higher level of Promoter A than Promoter B transcripts is a characteristic of osteosarcoma cancers.

Overall, transcript numbers per µg RNA in patient tissues for both Promoter A and Promoter B were lower than determined for SaOS-2 and U20S by approximately 10-fold or more (Table 5).

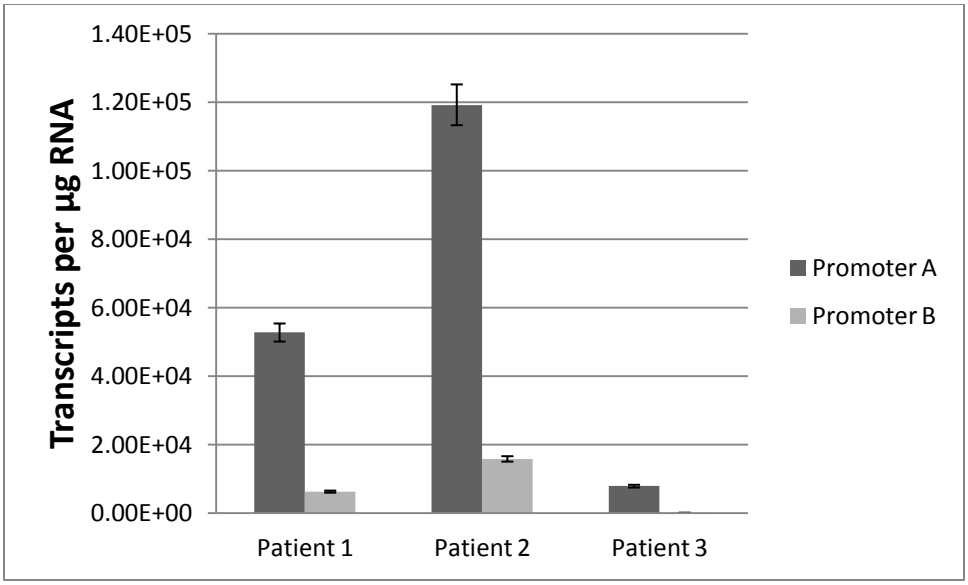

Figure 4. Higher Numbers of WNT5A Promoter A Transcripts in relation to Promoter B Transcripts in Patient Osteosarcoma Tumor Tissues. RNA was purchased and converted to cDNA. Promoter A and Promoter B transcripts were quantified by qRT-PCR using a standard curve. Standard error calculated from three technical replicas. WNT5A transcript copy numbers are expressed per µg of RNA.

Increased DNA Methylation of CpG Islands Associated with Promoter B in Osteosarcoma Cell Line U20S

It was previously shown in the lab that the decrease in Promoter B transcripts in SaOS-2 cells is associated with DNA methylation of particular sequences (Vaidya, 2013). We wanted to determine if DNA methylation was also involved in the decrease in Promoter B activity in U20S cells and how the pattern of DNA methylation compares to SaOS-2 cells. This is important as it may reveal sites of DNA methylation that are more prone to epigenetic modulation in osteosarcoma cancers. The methylation status of the six CpG islands shown in Figure 5A was analyzed through bisulfite sequencing. This was accomplished by using previously designed bisulfite sequencing specific primers that

amplify their respective CpG island in bisulfite modified DNA (Table 3; Vaidya, 2013). After bisulfite modification and amplification, the PCR products were subcloned and sequenced. The results of bisulfite sequencing are shown in Figure 5B.

The 27 CpGs of Region 1 CpG island were completely unmethylated in the five analyzed clones. Region 2 CpG island has 39 CpGs, but only the first 16 CpGs were able to be cloned in the six clones analyzed. The first 16 CpGs were unmethylated. Region 3 CpG island of 24 CpGs was found to be completely methylated in four of the six clones analyzed. The other two clones had only one unmethylated CpG out of the 24 CpGs. Region 4 CpG island has 27 CpGs but only CpGs 6-25 were able to be cloned. The CpGs 7-25 of Region 4 were shown to be methylated, but CpG 6 was unmethylated of the three clones analyzed. The CpG island Region 5 has 27 CpG's but only the first 22 CpGs were cloned. These 22 CpGs of Region 5 were methylated with the exception of CpG's 18 and 20, which were unmethylated of the four clones analyzed.

CpG Region 6 is associated with the Promoter B start of transcription and Exon 1β. It has 26 CpGs. Only two full length Region 6 clones were obtained and these were all unmethylated. We used a different primer set that amplified a region that includes only four of the CpG's in Region 6. Six of the nine clones obtained were found to be completely unmethylated, two were completely methylated, and one has three of the four CpG's methylated. Overall, these results indicate that U20S have some sequences associated with Promoter B that are methylated, which may contribute to the reduction in Promoter B transcript levels.

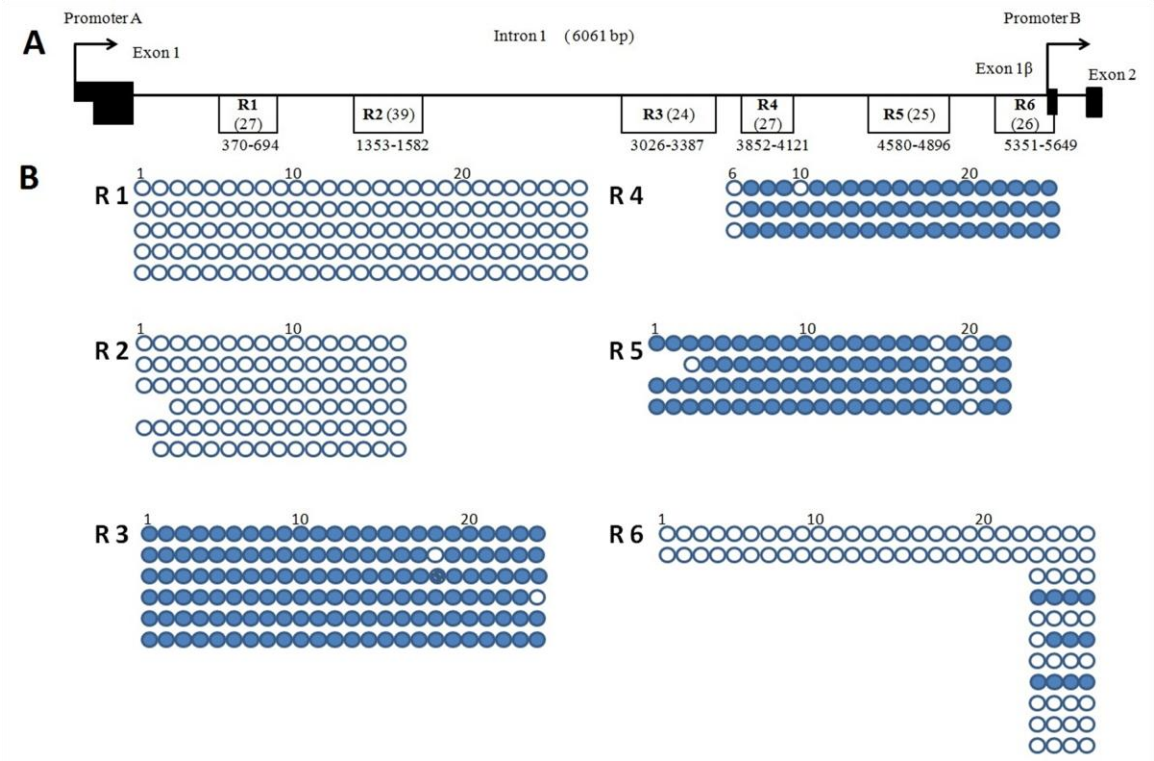

Figure 5. CpG Island Regions 1-6 and Methylation Status in U20S Osteosarcoma Cells. A. Location of CpG islands in WNT5A intron 1. R1-R6 are the CpG island regions with the number of CpG's in the sequence given in parentheses The numbers indicate relative base pair within the intron sequence with the first base pair of the intron as number 1. **B**. Results of bisulfite sequencing in U20S. Each circle represents a CpG within that particular CpG island region. Numbers correspond to the CpG relative location within the region. Closed circle = methylated CpG; open circle = unmethylated CpG. Each row is an individual sequenced clone.

Reduction in H3K4me3 Enrichment in Promoter B Region 6

Increased methylation was detected in Regions 3, 4, and 5 of U20S. However, Region 6, associated with the Promoter B start of transcription, was less methylated. Thus, the reduction in Promoter B activity in U20S may potentially be due to histone modifications and not primarily to DNA methylation. We used chromatin immunoprecipitation (ChIP) assay to examine Promoter A, Promoter B, and Regions 3, 4,

and 5 for enrichment of specific histone modifications. These included H3K27me3, H3K4me3, and H3K9me3. The histones H3K27me3 and H3K9me3 are repressive histone marks. H3K4me3 is an activating histone mark. As controls, we performed ChIP using anti-RNA polymerase II, which should be present in active promoters, and as a negative control that should not "pull-down" anything specific chromatin, anti IgG was performed in the ChIP assays. The locations of the primers used in ChIP are shown in Figure 6A. A GAPDH primer was also run with all ChIP assays as a highly expressed gene.

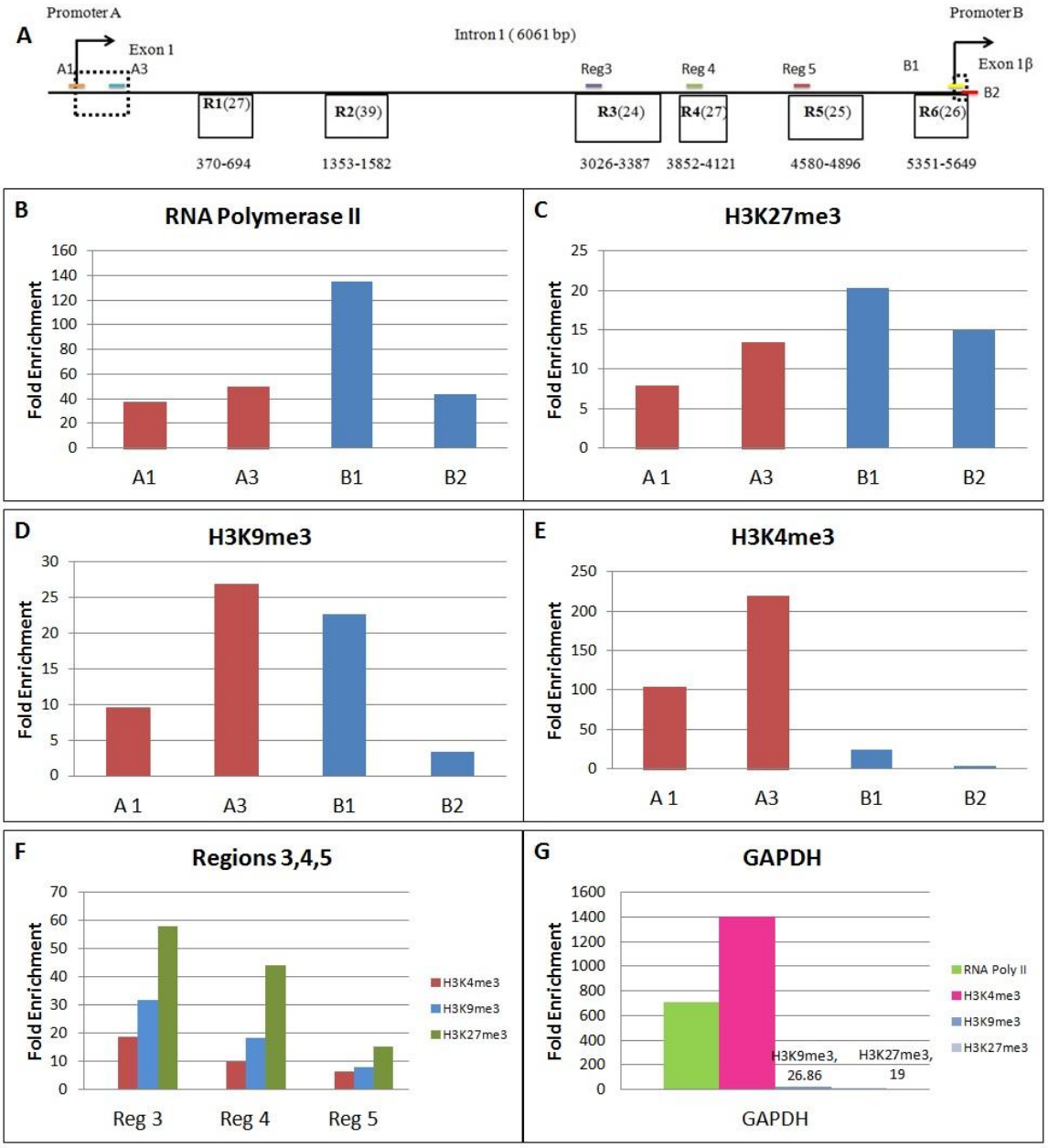

Figure 6. Chromatin Immunoprecipitation (ChIP) Assay of U20S Cells at the WNT5A Promoter A and Promoter B Genomic Region. A. The location of the ChIP primers for Promoter A, Promoter B and the Regions 3, 4, and 5. Fold enrichment for Promoter A and B probes of **B**. RNA polymerase II, **C**. H3K27me3, **D**. H3K9me3, **E**. H3K4me3. **F**. Fold enrichment of H3K4me3, H3K9me3 and H3K27me3 at Regions 3, 4, 5, **G**. Fold Enrichment for GAPDH.

RNA polymerase II was enriched on both Promoter A and Promoter B (Figure 6B). In fact, enrichment was greater using Promoter B primer B1 but it is likely that this is not significant, considering primer B2 overlaps B1. Also, greater enrichment would not be expected considering the lower levels of Promoter B activity in U20S. In comparison, the highly expressed GAPDH had much higher levels of RNA polymerase II enrichment than either Promoter A or B (Figure 6G; Table 6). This would be expected.

The repressive histone marks, H3K27me3 and H3K9me3, appeared equally enriched at both Promoters A and Promoter B (Figure 6C and D). The level of enrichment is similar to what is observed in GAPDH (Figure 6G; Table 6), therefore this likely represents levels that are unrelated to transcriptional inactivation.

In contrast, the active histone mark, H3K4me3, had higher levels of enrichment for Promoter A probes in comparison to the Promoter B probes (Figure 6E; Table 6). The GAPDH gene had high levels for H3K4me3 enrichment, which would be expected for a highly expressed gene (Figure 6G). These results suggest that H3K4me3 is reduced at the Promoter B Region 6.

The three histone marks, H3K27me3, H3K9me3 and H3K4me3 were examined in Regions 3, 4 and 5 (Figure 6F). Regions 3 and 4 had higher levels of enrichment of H3K27me3, even in comparison to GAPDH (Table 6). Region 5 had H3K27me3 enrichment levels similar to GAPDH. In relation to Promoter A, Promoter B and GAPDH, Regions 3, 4 and 5 had no enrichment of H3K9me3 (Table 6). For H3K4me3,

Regions 3, 4 and 5 had lower levels of enrichment more similar to Promoter B (Figure 6F; Table 6).

Table 6. Chromatin Immunoprecipitation (ChIP) Fold Enrichment Values of U20S and SaOS-2.

U20S								
	A1	A3	B1	B2	Reg 3	Reg 4	Reg 5	GAPDH
RNA polymerase II	37.22	49.73	135.24	43.71	_	_	_	713.93
H3K4me3	104.45	219.56	24.96	4.01	18.61	9.8	6.6	1402.82
H3K9me3	9.55	26.902	22.65	3.32	31.72	18.29	8.13	26.89
H3K27me3	7.91	13.39	20.28	14.9	57.85	44	15.42	19

SaOS-2					
	A1	A3	B1	B2	GAPDH
RNA polymerase II	5.32	5.74	2.97	4.17	2624.25
H3K27me3	1.48	0.25	2.52	1.46	10.83

In SaOS-2, we used ChIP to examine Promoter A and Promoter B for the repressive histone modification, H3K27me3 (Figure 7). The controls, anti-RNA polymerase II and IgG were also used in SaOS-2. GAPDH was run with the ChIP as a highly expressed gene (Figure 7D). The results of SaOS-2 have a similar pattern to the U20S results above except their enrichment levels are much lower than U20S. In SaOS-2, there were similar level of enrichment for RNA polymerase II for Promoter A and Promoter B (Figure 7B). For H3K27me3, the Promoter B probes primer B1 and B2 showed some, but low enrichment, whereas the Promoter A probes show essentially no enrichment (Figure 7C). Enrichment of H3K27me3 for Promoter A would not be expected due to the higher activity level of Promoter A in SaOS-2. A higher enrichment

level of H3K27me3 on Promoter B Region 6 might be expected. GAPDH had very high levels of RNA polymerase II enrichment and some enrichment for H3K27me3 (Figure 7D; Table 6). The results suggest there was no enrichment for H3K27me3 at either Promoters A or B.

It is not clear why enrichment levels were overall so low for the WNT5A genomic region in SaOS-2, considering the values for GAPDH were similar to U20S. A possible answer to the low enrichment values for SaOS-2 could be the DNA methylation and steric hindrance to antibody binding. Histone tails serve as docking sites for transcription factors or other modifying enzymes. The binding of these proteins could block access of the antibody for a histone modification (Collas, 2010). Also the tight packaging of histones could block an antibody from binding to a targeted histone modification (Kimura, 2013).

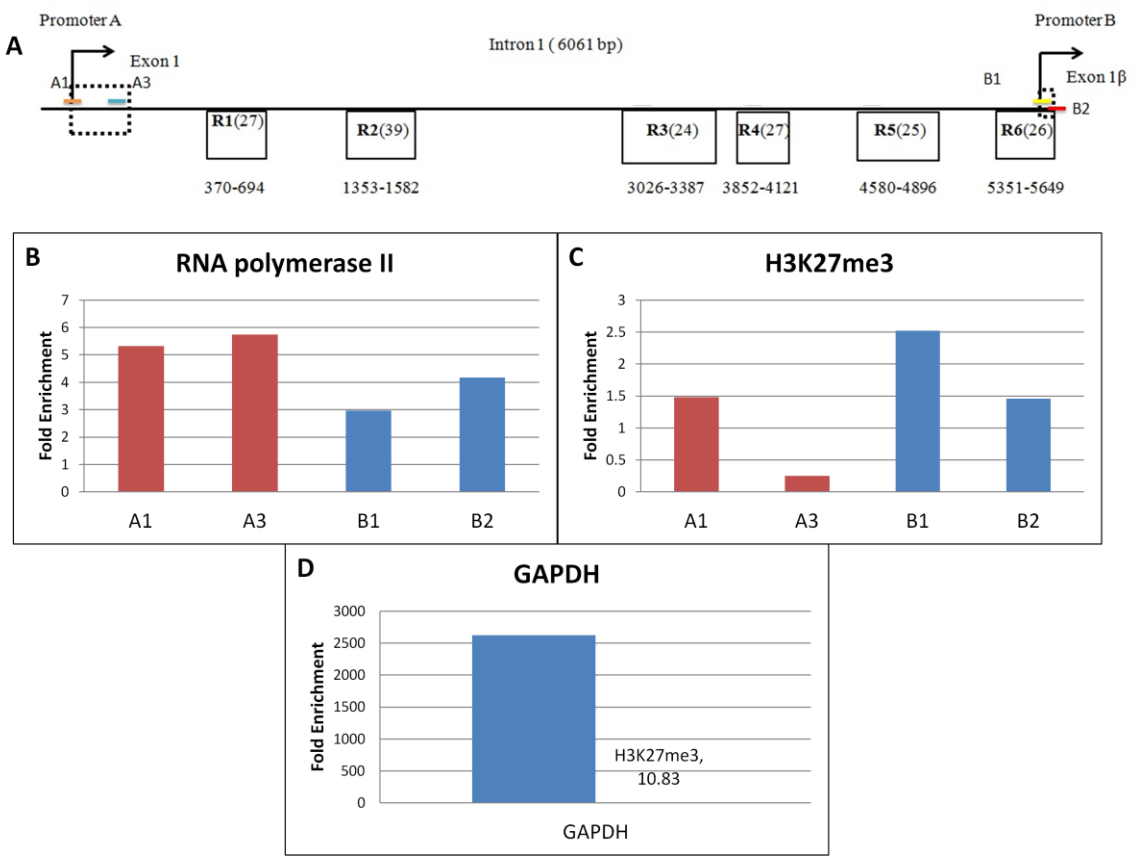

Figure 7. Chromatin Immunoprecipitation (ChIP) Assay of SaOS-2 Cells at the WNT5A Promoter A and Promoter B Genomic Region. A. The location of the primer probes for Promoter A and Promoter B. Fold enrichment for Promoter A and B probes as **B**. RNA polymerase II, **C**. H3K27me3, **D**. GAPDH.

CHAPTER IV

DISCUSSION

Summary of Major Findings

In this study, the *WNT5A* Promoter A and Promoter B transcript levels were examined in the U20S osteosarcoma cell line and patient osteosarcoma tumor tissue samples. Our results suggest that a decrease in Promoter B transcripts in relation to Promoter A transcripts is a feature of osteosarcoma cancers. The DNA methylation status of six CpG islands that may be associated with Promoter B transcription was determined. The results showed that Regions 1 and 2 were completely unmethylated. Regions 3, 4, and 5 were highly methylated, whereas Region 6, which includes the transcription start site of Promoter B, was less methylated in comparison to SaOS-2 cells. The level of methylation was negatively correlated with Promoter B transcription. This results indicates that methylation of Region 6 may not be the underlying cause of the reduction in Promoter B transcript levels. Chromatin immunoprecipitation (ChIP) analysis suggests that the repressive histone marks, H3K9me3 and H3K27me3, are similar between the Promoter A and Promoter B regions. Significantly, Promoter A is more enriched in the active histone mark, H3K4me3 than Promoter B. These results indicate that histone modifications and DNA methylation are contributing to the reduction of Promoter B activity in U20S cells.

Decreased Promoter B Transcripts in Osteosarcoma Cell Lines and Primary Osteosarcoma Tissues

WNT5A is a key protein involved in maturation of osteoblasts and thus it is expected to be involved in osteosarcoma. WNT5A has been shown to be expressed in osteosarcomas. In SaOS-2 and U20S, it has been found that constitutively active WNT5A signaling increased MMP-13 activation and invadopodia formation that leads to cell invasion in these cancer cells (Enomoto et al., 2009). More recently, WNT5A has been shown to promote migration of human osteosarcoma cells through the phosphatidylinositol-3 kinase/Akt signaling pathway (Zhang et al 2014). These studies clearly support the conclusion that WNT5A has oncogenic activities in osteosarcoma cells. However, in these studies the focus was on the transcripts derived from Promoter A and its protein product.

In our lab, the transcript levels from the WNT5A Promoters A and B were analyzed in osteoblasts and SaOS-2 osteosarcoma. In normal osteoblasts, Promoter B transcripts were higher in comparison to Promoter A transcripts (Hsu, 2012). The A to B transcript ratio was 0.09 (± 0.02) (Table 5). These results suggest that in normal osteoblast Promoter B is more active. In contrast to osteoblasts, SaOS-2 osteosarcoma cells had Promoter A transcripts similar to or slightly higher than in osteoblast cells, whereas Promoter B transcripts were greatly reduced (Hsu, 2012). The ratio of A to B was 224.5 (±65.2) (Table 5). Hence, Promoter B transcript numbers were approximately 2000 times higher in normal osteoblast cell than in SaOS-2 osteosarcoma cells.

Corresponding protein levels for Promoter A and Promoter B are not known. Differentiation between Promoter A and Promoter B protein isoforms requires antibodies specific to each isoform.

In this study, we analyzed Promoter A and B transcript levels in U20S cells to determine if the decrease in Promoter B is a characteristic of osteosarcoma cell lines. The Promoter A transcripts were $9.7x10^5$ (per µg of RNA), which is lower than in normal osteoblasts and SaOS-2 cells. Promoter B transcripts were $1.1x10^5$ (per µg RNA), which were higher than Promoter B transcripts in SaOS-2 but lower than transcripts numbers in normal osteoblasts. The A to B ratio for U20S was 11.9 (±4.1) (Table 5). Promoter B transcripts in normal osteoblasts are about 500 times higher than in U20S cells. Overall, these results suggest that a reduction in Promoter B is common to osteosarcoma cell lines.

It was important to determine if the reduction in Promoter B transcript levels is common in primary osteosarcoma tumor tissue. RNA from three different patient tumor tissues were purchased and analyzed for WNT5A Promoter A and Promoter B transcripts. All three patient tumor tissue samples had lower levels of Promoter B in comparison to Promoter A transcripts. Patients 1 and 2 had an A to B ratio of 9.2 and 7.5, respectively. Patient 3 had an A to B ratio of 78.5. Patients 1 and 2 had an A to B ratio similar to the U20S cell line. Patient 3 had an A to B ratio more similar to SaOS-2 cell line.

The absolute levels of WNT5A promoter A and B transcripts per µg RNA in the primary tumor tissues is relatively low, in comparison to the cell lines. For example, patients 1 and 3 had only $5x10^4$ and $8x10^3$ transcripts per µg RNA of Promoter A transcripts, respectively (Table 5). Patient 2 had a higher level at $1x10^5$ per µg RNA but still less by nearly 10 fold as in U20S. The lower levels of transcripts per µg of RNA are likely due to the tumor tissue including other cell types.

It is of potential significance that Patient 2 RNA was isolated from a metastatic osteosarcoma and the levels of both Promoter A and B transcripts were higher in this sample. However, the A to B ratio was lowest of the three tissues. As previously discussed, high levels of WNT5A Promoter A isoforms can induce cellular characteristics of metastasis in osteosarcoma cells.

Patient 1 had a humerus parosteal osteosarcoma and Patient 3 had a recurrent osteosarcoma. Both these patients had lower Promoter A and Promoter B transcripts than Patient 2. Patient 2 had a metastatic osteosarcoma and had higher levels of Promoter A and Promoter B transcripts in comparison to the other patient tissues. Looking at the transcript numbers and types of cancers from each patient, there may be a decrease in Promoter B as the osteosarcoma cancer progresses.

Overall, results with, U20S, SaOS-2, patient tumor tissue and normal osteoblasts suggests that during cancer progression in osteosarcoma, Promoter B is being inactivated.

Aberrant DNA Methylation of *WNT5A* Intron 1 CpG Islands in U20S Osteosarcoma Cells

Previous bisulfite sequencing was conducted on *WNT5A* CpG islands located in intron 1 in osteoblast and SaOS-2 osteosarcoma cells in our lab. In osteoblast, all CpG island Regions 1 to 6 were completely unmethylated (Vaidya, 2013). In SaOS-2, Regions 1 and 2 were completely unmethylated. Regions 3, 4 and 5 were completely methylated in SaOS-2. Region 6 was partially methylated in SaOS-2. In SaOS-2, only one full Region 6 clone was sequenced. This clone was unmethylated for CpGs 1-15 and methylated at CpGs 16-26. However, using a different primer set that amplified CpGs 23-26 in Region 6, ten clones were sequenced of SaOS-2. Of these ten clones, five were completed methylated, four were completely unmethylated, one showed a single unmethylated CpG of the four CpGs (Figure 8).

In this study, we found similar results in U20S. Regions 1 and 2 were completely unmethylated. Regions 3, 4 and 5 were mostly methylated yet a few CpGs in each region were unmethylated. This similarity between U20S and SaOS-2 suggest that sites of DNA methylation during osteosarcoma progression are unique to this cancer type. Region 6 had differing levels of methylation especially at CpGs 23-26. As a comparison in Region 6, SaOS-2 was 61.4% methylated in CpGs 23-26, whereas U20S was 25% methylated based on the all clones that were sequenced (Figure 8). These results show that the Promoter B start of transcription and Exon 1β region are less methylated in U20S osteosarcoma than in SaOS-2. The level of methylation at Region 6 is negatively

correlated with Promoter B activity. We found that Promoter B is more active in U20S cells, in comparison to SaOS-2 cells and U20S cells is less methylated in Region 6. This relationship suggests that even low methylation in Region 6 may influence Promoter B transcription levels.

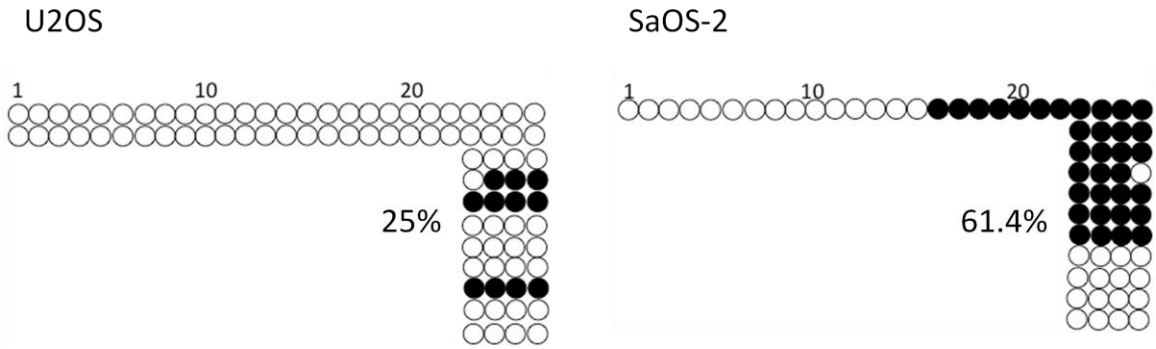

Figure 8. Methylation Status in U20S and SaOS-2 CpG Island Region 6. Each circle represents a CpG within that particular CpG island region. The numbers indicate relative base pair within the intron sequence with the first base pair of the intron as number 1. Numbers correspond to the CpG location within the region. Percent are methylated CpGs divided by total CpGs in CpGs 23-26 of all clones. Closed circle = methylated CpG; open circle = unmethylated CpG. Each row is an individual sequenced clone.

Regions 1 and 2 in osteosarcoma are possibly unmethylated due to its proximity to the Promoter A Exon 1 (Figure 5). Regions 3, 4 and 5 may or may not be involved in the regulation of Promoter B. The results of Vaidya (2013) do not provide a clear answer. When SaOs-2 cells were treated with 5-aza-deoxycytidine, which removes methyl groups from DNA, the level of Promoter B transcripts increased dramatically. Bisulfite sequencing showed that few of the methylated groups in Region 3, 4, 5 and 6 were altered. It would be expected that more CpGs would be demethylated in Region 6, but this was not the case.

It is puzzling that U20S cells have such low levels of methylation in Region 6 CpGs 23-26. Although the number of Promoter B transcripts (per µg of RNA) is higher in U20S cells in comparison to SaOS-2 cells, transcript levels are reduced relative to normal osteoblasts. This suggests that Promoter B transcription is reduce in U20S in spite of the lower level of methylation in Region 6. Another possibility is that methylation of Regions 3, 4, or 5 is also impacting U20S Promoter B transcription, as these regions may include enhancers. Also, as our results show changes in histone modifications is likely contributing to reduced Promoter B transcription.

Reduced H3K4me3 in Promoter B Region 6 of U20S Cells

Three different histone modifications, H3K4me3, H3K9me3 and H3K27me3 were examined for enrichment at Promoter A, Promoter B, and Regions 3, 4, 5 (Figures 6 and 7). RNA polymerase II was used as a positive control for actively transcribed genes. A GAPDH primer was included in the ChIP assay as a gene that is highly expressed.

H3K27me3 is associated with transcriptional repression and promotes chromatin compaction (Rose & Klose, 2014). In somatic and cancer cells, H3K27me3 was found to overlap with areas of DNA methylation (Schlesinger et al., 2007; Brinkman et al., 2012). One prediction is that Promoter A region of SaOS-2 and U20S cells would be less enriched in H3K27me3 than Promoter B. Also, Regions 3, 4 and 5 would be enriched in H3K27me3. Our results show no difference in H3K27me3 enrichment between Promoter A and Promoter B in U20S or in SaOS-2. Regions 3 and 4 had higher levels of enrichment in H3K27me3 in comparison to GAPDH. These results indicate that

H3K27me3 is not responsible for the reduction in Promoter B activity in U20S or SaOS-2.

H3K9me3 is generally associated with repressed chromatin and has a role in de novo methylation of heterochromatin regions (Gordon et al. 2013). It would not be expected to associate with Promoters A and B but may possibly be associated with Regions 3, 4 and 5. The results show that H3K9me3 is not more enriched at Promoter A and Promoter B than measured at GAPDH in U20S cells. This finding suggests that H3K9me3 is not associated with the decrease in Promoter B expression in U20S cells. Region 3, 4 and 5 show no greater enrichment in H3K9me3 than GAPDH, indicating these sequence regions are not heterochromatic.

H3K4me3 is associated with active promoters and is found in regions of unmethylated DNA (Rose & Klose, 2014). It would be predicted that H3K4me3 would be more enriched at Promoter A than Promoter B and not associated with Regions 3, 4, and 5. H3K4me3 showed higher enrichment in Promoter A than Promoter B of U20S cells. The reduction in H3K4me3 at Promoter B could, in part, explain the decrease in Promoter B activity in U20S cells. A possible mechanism is that with reduced H3K4me3, the DNA methyltransferase Dnmt3 a/b, could de novo methylate CpGs in the Region 6. It appears as if the U20S Promoter B Region 6 is in the process of being de novo methylated. Regions 3, 4, 5 had low levels of H3K4me3 enrichment similar to Promoter B and lower than Promoter A. As expected, GAPDH had high levels of H3K4me3 enrichment.

Both Promoter A and B are active in the U20S cells, so some RNA polymerase II is expected to be binding to these promoters. Overall our results confirm this prediction, although the Promoter B B1probe gave a higher value of enrichment. RNA polymerase II was, as expected, highly enriched for GAPDH.

In the SaOS-2 cells we found that H3K27me3 is not enriched in either Promoters A or B. These results are consistent with the U20S results.

The U20S ChIP data results suggest that the loss of H3K4me3is involved in the decrease in Promoter B transcripts. There seems to be a decrease in H3K4me3 when moving across the WNT5A intron 1. In Promoter A, there was enrichment of H3k4me3 (Figure 6E). In Regions 3, 4, 5, there is a progressive decrease in H3K4me3 enrichment (Figure 6F). There are lower levels of H3K4me3 enrichment at Promoter B than at the Promoter A region (Figure 6E). A possible model for the decrease in Promoter B transcripts is the loss of methylation at H3K4 leads to both a decrease in transcription factor recruitment and increased DNA methylation through the binding of DNA methyltransferases (Figure 9). The loss of H3K4 methylation at the Promoter B region could then lead to the DNA methylation patterns seen in Figure 5 for Regions 3, 4, 5 and 6 of U20S. The combination of H3K4 methylation loss and DNA methylation could be the reason for the decrease in Promoter B transcripts.

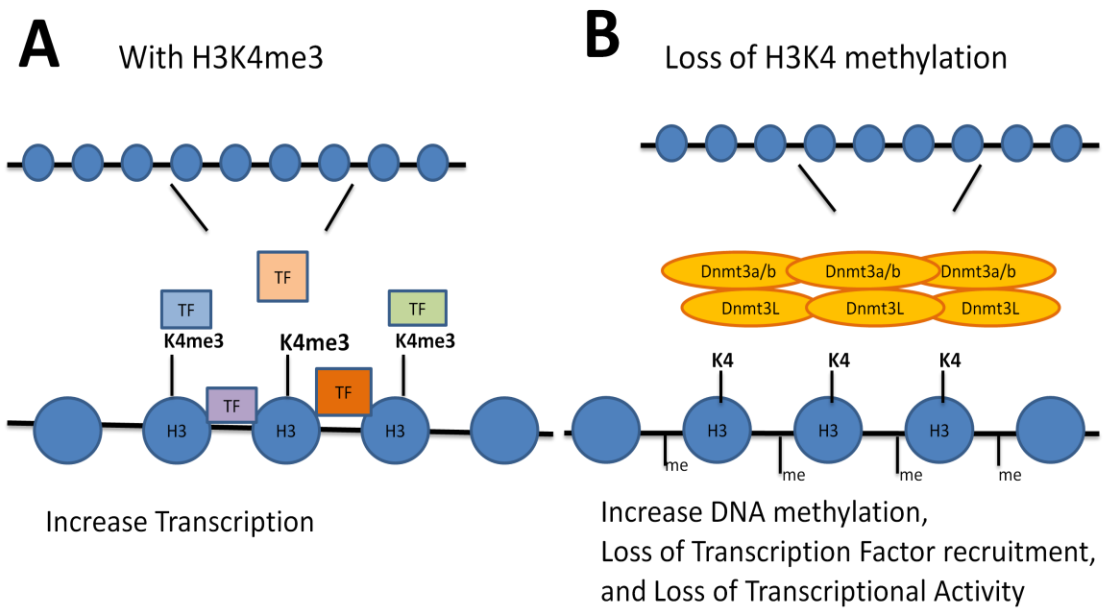

Figure 9. Model for Histone Modification and DNA Methylation related to Promoter B Transcription. **A**. The methylation of H3K4me3 leads to the recruitment of transcription factors (TF). This then leads to an increase in transcription through the recruitment of RNA polymerase II and other transcriptional elements. **B**. The loss of H3K4me3 allows for the binding of DNA methyltransferase 3L (Dnmt 3L), which forms a complex with DNA methyltransferase 3a/b (Dnmt3a/b). The Dnmt complex then methylates the DNA, blocking transcription.

Overall, the ChIP assays suggest that a reduction in the activating histone, H3K4me3 at the Promoter B Region 6, is associated with reduced Promoter B activity. It may also be responsible for the increased DNA methylation at Region 6. It will be important to complete the ChIP assay in SaOS-2 to confirm that Promoter B lacks H3K4me3. This does not explain the methylation of Regions 3, 4 and 5 and their role, if any, in regulating WNT5A Promoter A and Promoter B expression. Nor do these findings reveal the functional role of the WNT5A Promoter B protein isoform in osteoblast cell function.

REFERENCES

Bauer, M., Bénard, J., Gaasterland, T., Willert, K., & Cappellen, D. (2013). WNT5A encodes two isoforms with distinct functions in cancers. *PloS One*, *8*(11), e80526. doi:10.1371/journal.pone.0080526

Bo, H., Zhang, S., Gao, L., Chen, Y., Zhang, J., Chang, X., & Zhu, M. (2013). Upregulation of Wnt5a promotes epithelial-to-mesenchymal transition and metastasis of pancreatic cancer cells. *BMC Cancer*, *13*(1), 496. doi:10.1186/1471-2407-13-496

Bostick, M., Kim, J. K., Estève, P.-O., Clark, A., Pradhan, S., & Jacobsen, S. E. (2007). UHRF1 plays a role in maintaining DNA methylation in mammalian cells. *Science (New York, N.Y.)*, *317*(5845), 1760–4. doi:10.1126/science.1147939

Bradley, E. W., & Drissi, M. H. (2010). WNT5A regulates chondrocyte differentiation through differential use of the CaN/NFAT and IKK/NF-kappaB pathways. *Molecular Endocrinology (Baltimore, Md.)*, *24*(8), 1581–93. doi:10.1210/me.2010-0037

Brinkman, A. B., Gu, H., Bartels, S. J. J., Zhang, Y., Matarese, F., Simmer, F., … Stunnenberg, H. G. (2012). Sequential ChIP-bisulfite sequencing enables direct genome-scale investigation of chromatin and DNA methylation cross-talk. *Genome Research*, *22*(6), 1128–38. doi:10.1101/gr.133728.111

Cedar, H., & Bergman, Y. (2009). Linking DNA methylation and histone modification: patterns and paradigms. *Nature Reviews. Genetics*, *10*(5), 295–304. doi:10.1038/nrg2540

Clevers, H. (2006). Wnt/beta-catenin signaling in development and disease. *Cell*, *127*(3), 469–80. doi:10.1016/j.cell.2006.10.018

Collas, P. (2010). The current state of chromatin immunoprecipitation. *Molecular Biotechnology*, *45*(1), 87–100. doi:10.1007/s12033-009-9239-8

Ekström, T., Lennartsson, A., & Ekwall, K. (2009). Histone modification patterns and epigenetic codes. *Biochimica et Biophysica Acta (BBA) - General Subjects*, *1790*(9),

863–868. Retrieved from http://www.sciencedirect.com/science/article/pii/S0304416509000038

Enomoto, M., Hayakawa, S., Itsukushima, S., Ren, D. Y., Matsuo, M., Tamada, K., … Minami, Y. (2009). Autonomous regulation of osteosarcoma cell invasiveness by Wnt5a/Ror2 signaling. *Oncogene*, *28*(36), 3197–208. doi:10.1038/onc.2009.175

Gordon, C. A., Hartono, S. R., & Chédin, F. (2013). Inactive DNMT3B splice variants modulate de novo DNA methylation. *PloS One*, *8*(7), e69486. doi:10.1371/journal.pone.0069486

Guenther, M. G., Levine, S. S., Boyer, L. A., Jaenisch, R., & Young, R. A. (2007). A chromatin landmark and transcription initiation at most promoters in human cells. *Cell*, *130*(1), 77–88. doi:10.1016/j.cell.2007.05.042

Hsu, Chia-Chi, Katula, K. (2012). *HSU, CHIA-CHI, M.S. Expression ofWnt5a Alternative Promoters A and B During Cancer Progression and Cellular Differentiation*. Univeristy of North Carolina at Greensboro. Retrieved from http://libres.uncg.edu/ir/uncg/listing.aspx?id=8641

Huang, Y., Liu, G., Zhang, B., Xu, G., Xiong, W., & Yang, H. (2010). Wnt-5a regulates proliferation in lung cancer cells. *Oncology Reports*, *23*(1), 177–81. Retrieved from http://www.ncbi.nlm.nih.gov/pubmed/19956879

Katula, K. S., Joyner-Powell, N. B., Hsu, C.-C., & Kuk, A. (2012). Differential regulation of the mouse and human Wnt5a alternative promoters A and B. *DNA and Cell Biology*, *31*(11), 1585–97. doi:10.1089/dna.2012.1698

Kikuchi, A., Yamamoto, H., Sato, A., & Matsumoto, S. (2012). Wnt5a: its signalling, functions and implication in diseases. *Acta Physiologica (Oxford, England)*, *204*(1), 17–33. doi:10.1111/j.1748-1716.2011.02294.x

Kimura, H. (2013). Histone modifications for human epigenome analysis. *Journal of Human Genetics*, *58*(7), 439–45. doi:10.1038/jhg.2013.66

Kurayoshi, M., Oue, N., Yamamoto, H., Kishida, M., Inoue, A., Asahara, T., … Kikuchi, A. (2006). Expression of Wnt-5a is correlated with aggressiveness of gastric cancer by stimulating cell migration and invasion. *Cancer Research*, *66*(21), 10439–48. doi:10.1158/0008-5472.CAN-06-2359

Li, Q., & Chen, H. (2012). Silencing of Wnt5a during colon cancer metastasis involves histone modifications. *Epigenetics : Official Journal of the DNA Methylation Society*, *7*(6), 551–8. doi:10.4161/epi.20050

Liang, H., Chen, Q., Coles, A. H., Anderson, S. J., Pihan, G., Bradley, A., … Jones, S. N. (2003). Wnt5a inhibits B cell proliferation and functions as a tumor suppressor in hematopoietic tissue. *Cancer Cell*, *4*(5), 349–360. Retrieved from http://www.sciencedirect.com/science/article/pii/S153561080300268X

MacDonald, B. T., Tamai, K., & He, X. (2009). Wnt/beta-catenin signaling: components, mechanisms, and diseases. *Developmental Cell*, *17*(1), 9–26. doi:10.1016/j.devcel.2009.06.016

Maeda, K., Kobayashi, Y., Udagawa, N., Uehara, S., Ishihara, A., Mizoguchi, T., … Takahashi, N. (2012). Wnt5a-Ror2 signaling between osteoblast-lineage cells and osteoclast precursors enhances osteoclastogenesis. *Nature Medicine*, *18*(3), 405–12. doi:10.1038/nm.2653

Martín, V., Valencia, A., Agirre, X., Cervera, J., San Jose-Eneriz, E., Vilas-Zornoza, A., … Román-Gómez, J. (2010). Epigenetic regulation of the non-canonical Wnt pathway in acute myeloid leukemia. *Cancer Science*, *101*(2), 425–32. doi:10.1111/j.1349-7006.2009.01413.x

Matsumoto, S., Fumoto, K., Okamoto, T., Kaibuchi, K., & Kikuchi, A. (2010). Binding of APC and dishevelled mediates Wnt5a-regulated focal adhesion dynamics in migrating cells. *The EMBO Journal*, *29*(7), 1192–204. doi:10.1038/emboj.2010.26

Mitra, S. K., Hanson, D. A., & Schlaepfer, D. D. (2005). Focal adhesion kinase: in command and control of cell motility. *Nature Reviews. Molecular Cell Biology*, *6*(1), 56–68. doi:10.1038/nrm1549

Nishita, M., Enomoto, M., Yamagata, K., & Minami, Y. (2010). Cell/tissue-tropic functions of Wnt5a signaling in normal and cancer cells. *Trends in Cell Biology*, *20*(6), 346–354. Retrieved from http://www.sciencedirect.com/science/article/pii/S0962892410000528

Pourreyron, C., Reilly, L., Proby, C., Panteleyev, A., Fleming, C., McLean, K., … Foerster, J. (2012). Wnt5a is strongly expressed at the leading edge in non-melanoma skin cancer, forming active gradients, while canonical Wnt signalling is repressed. *PloS One*, *7*(2), e31827. doi:10.1371/journal.pone.0031827

Ripka, S., König, A., Buchholz, M., Wagner, M., Sipos, B., Klöppel, G., … Michl, P. (2007). WNT5A--target of CUTL1 and potent modulator of tumor cell migration and invasion in pancreatic cancer. *Carcinogenesis*, *28*(6), 1178–87. doi:10.1093/carcin/bgl255

Rose, N. R., & Klose, R. J. (2014). Understanding the relationship between DNA methylation and histone lysine methylation. *Biochimica et Biophysica Acta*. doi:10.1016/j.bbagrm.2014.02.007

Sansom, O. J., Reed, K. R., van de Wetering, M., Muncan, V., Winton, D. J., Clevers, H., & Clarke, A. R. (2005). Cyclin D1 is not an immediate target of beta-catenin following Apc loss in the intestine. *The Journal of Biological Chemistry*, *280*(31), 28463–7. doi:10.1074/jbc.M500191200

Schlesinger, Y., Straussman, R., Keshet, I., Farkash, S., Hecht, M., Zimmerman, J., … Cedar, H. (2007). Polycomb-mediated methylation on Lys27 of histone H3 pre-marks genes for de novo methylation in cancer. *Nature Genetics*, *39*(2), 232–6. doi:10.1038/ng1950

Ten Berge, D., Brugmann, S. A., Helms, J. A., & Nusse, R. (2008). Wnt and FGF signals interact to coordinate growth with cell fate specification during limb development. *Development (Cambridge, England)*, *135*(19), 3247–57. doi:10.1242/dev.023176

Vaidya, Himani. *Role of DNA Methylation in WNT5A Promoter B Expression in Osteosarcoma Cells.* Thesis. University of North Carolina at Greensboro, 2013. Greensboro: UNCG, 2013. Print.

Wang, Q., Symes, A. J., Kane, C. A., Freeman, A., Nariculam, J., Munson, P., … Ahmed, A. (2010). A novel role for Wnt/Ca2+ signaling in actin cytoskeleton remodeling and cell motility in prostate cancer. *PloS One*, *5*(5), e10456. doi:10.1371/journal.pone.0010456

Weeraratna, A. T., Jiang, Y., Hostetter, G., Rosenblatt, K., Duray, P., Bittner, M., & Trent, J. M. (2002). Wnt5a signaling directly affects cell motility and invasion of metastatic melanoma. *Cancer Cell*, *1*(3), 279–288. doi:10.1016/S1535-6108(02)00045-4

Wong, H.-C., Bourdelas, A., Krauss, A., Lee, H.-J., Shao, Y., Wu, D., … Zheng, J. (2003). Direct binding of the PDZ domain of Dishevelled to a conserved internal sequence in the C-terminal region of Frizzled. *Molecular Cell*, *12*(5), 1251–60. Retrieved from http://www.ncbi.nlm.nih.gov/pubmed/14636582

Yamaguchi, T. P., Bradley, A., McMahon, A. P., & Jones, S. (1999). A Wnt5a pathway underlies outgrowth of multiple structures in the vertebrate embryo. *Development (Cambridge, England)*, *126*(6), 1211–23. Retrieved from http://www.ncbi.nlm.nih.gov/pubmed/10021340

Yamamoto, H., Oue, N., Sato, A., Hasegawa, Y., Matsubara, A., Yasui, W., & Kikuchi, A. (2010). Wnt5a signaling is involved in the aggressiveness of prostate cancer and expression of metalloproteinase. *Oncogene*, *29*(14), 2036–46. doi:10.1038/onc.2009.496

Yang, D.-H., Yoon, J.-Y., Lee, S.-H., Bryja, V., Andersson, E. R., Arenas, E., … Choi, K.-Y. (2009). Wnt5a is required for endothelial differentiation of embryonic stem cells and vascularization via pathways involving both Wnt/beta-catenin and protein kinase Calpha. *Circulation Research*, *104*(3), 372–9. doi:10.1161/CIRCRESAHA.108.185405

Ying, J., Li, H., Yu, J., Ng, K. M., Poon, F. F., Wong, S. C. C., … Tao, Q. (2008). WNT5A exhibits tumor-suppressive activity through antagonizing the Wnt/beta-catenin signaling, and is frequently methylated in colorectal cancer. *Clinical Cancer Research : An Official Journal of the American Association for Cancer Research*, *14*(1), 55–61. doi:10.1158/1078-0432.CCR-07-1644